

**EFFECT OF MOISTURE CONTENT ON THE DESORPTION
OF CARBON TETRACHLORIDE FROM HANFORD SILT**

By

SACHIN MERVIN SALDANHA

A thesis submitted in partial fulfillment of
the requirements for the degree of

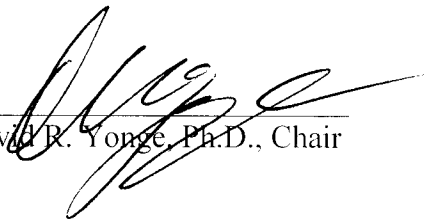
MASTER OF SCIENCE IN ENVIRONMENTAL ENGINEERING

WASHINGTON STATE UNIVERSITY
Department of Civil and Environmental Engineering

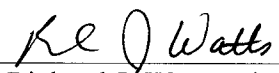
May 2009

To the Faculty of Washington State University:

The members of the Committee appointed to examine the thesis of **SACHIN MERVIN SALDANHA** find it satisfactory and recommend that it be accepted.



David R. Yonge, Ph.D., Chair



Richard J. Watts, Ph.D



Jeremy A. Rentz, Ph.D

ACKNOWLEDGEMENT

I would like to acknowledge my father, Walter Saldanha and mother, Winnie Saldanha. You taught me the importance of hard work and diligence. Your sacrifices helped me get to where I am today.

I would like to acknowledge my sisters, Sonia Saldanha and Shamila Saldanha and my brother, Santosh Saldanha for their love and support. I am grateful for having you as my family.

I would like to thank Dr. David Yonge for the opportunity to work with him and for his cooperation, understanding, and support throughout this process. I would not have finished had you not worked with me as diligently as you did. And in particular, thank you for all the patience as I figured my way around the lab.

I would like to thank Ms. Diana Washington for her constant support and assistance in the laboratory and with my research. I would like to thank Dr. Richard Watts and Dr. Jeremy Rentz for their guidance and time.

A special thanks to Clifton Alan Gray, mentor, friend, and colleague. Thank you for believing in me and giving me the opportunity to prove myself.

**EFFECT OF MOISTURE CONTENT ON THE DESORPTION
OF CARBON TETRACHLORIDE FROM HANFORD SILT**

Abstract

by Sachin Mervin Saldanha, M.S.
Washington State University
May 2009

Chair: David R. Yonge

The manufacture of plutonium at the Hanford Nuclear Reservation site in Richland, WA, resulted in the contamination of the vadose zone with carbon tetrachloride among other contaminants. Carbon tetrachloride, used as a solvent in the recovery of plutonium, was disposed of in unlined trenches and made its way into the subsurface. Although most of the contamination occurred in the late seventies, cleanup using soil vapor extraction (SVE) in the vadose zone began only in 1992. For SVE operations, the efficiency lowered significantly within a few weeks after initial high recoveries and resulted in high operation costs. The latest update on cleanup operations at Hanford states that approximately 78,000 Kg of the carbon tetrachloride has been removed from the vadose zone. In addition 24,000 lbs of carbon tetrachloride have been removed from the groundwater using pump and treat systems.

Several independent studies conducted indicate that the prolonged cleanup times are a result of the rate limited intra-particle diffusion of carbon tetrachloride from the vadose zone. This thesis investigates the impact of moisture content on the cleanup of carbon tetrachloride from Hanford silt. Several SVE experiments were conducted in a simulated vadose zone environment comprising a silt lens (10 cm x 20 cm x 10 cm)

embedded in sand within a 2.44m x 0.61m x 0.152m stainless steel box. The moisture content of the silt was varied (2%, 7% and 14%), while the quantity of liquid carbon tetrachloride (50 mL in the center of the silt lens) and airflow through the system (309 mL/min) were kept constant.

The results do not present conclusive evidence to suggest that the presence of moisture has an impact on the removal of adsorbed carbon tetrachloride. There was no evidence either of any effect of the presence of moisture on the removal of carbon tetrachloride from the pure phase. When the pure phase had been depleted, removal rates were slightly higher at lower moisture contents and lower concentrations of carbon tetrachloride vapors were measured in the exit stream over the same time period.

With the understanding that the rate of diffusion through water is slower than diffusion through air, it is likely that the presence of water decreases the rate of diffusion. The slow desorption of carbon tetrachloride and the subsequent lengthy cleanup times may also be a result of the intra-particle adsorption and diffusion.

TABLE OF CONTENTS

TABLE OF CONTENTS.....	vi
LIST OF TABLES.....	viii
LIST OF FIGURES	ix
1.0 INTRODUCTION	1
1.1 HANFORD SITE.....	3
1.1.1 Site Characterization.....	4
1.1.2 Contamination Inventory	5
1.2 DIFFICULTIES WITH THE CURRENT THEORY.....	7
1.3 OBJECTIVE	8
2.0 LITERATURE REVIEW	9
2.1 LABORATORY STUDIES.....	11
2.1.1 Effects of Soil Moisture.....	11
2.1.2 Effect of Soil Structure	13
2.1.3 Various Forces that Facilitate Transport.....	15
2.1.4 Effect of Hysteresis.....	17
2.2 SUMMARY	19
3.0 EXPERIMENTAL METHODS.....	20
3.1 VACUUM EXTRACTION CELL	20
3.1.1 Design	20
3.1.2 Setup and Operation.....	22
3.2 TEST RUN CONDITIONS	25
3.2.1 Flow rate, Temperature, and Relative Humidity	26
3.3 SAMPLING PROCEDURE	26
3.4 MOISTURE CONTENT OF SILT LENS.....	29
3.4.1 Measuring Residual Moisture Content	29
3.4.2 Increasing the Moisture Content of the Silt Lens	30
3.5 SAMPLE ANALYSIS	30
3.5.1 Analysis with the TCD.....	32
3.5.2 Analysis with the FID	33
3.5.3 Analysis with the ECD.....	33

3.6	TRACER GAS TESTS	34
3.7	HEALTH AND SAFETY PRECAUTIONS	35
4.0	RESULTS AND DISCUSSIONS.....	37
4.1	VAPOR EXTRACTION CELL	37
4.2	EFFLUENT CONCENTRATION DATA	38
4.3	DATA DISCUSSION FOR EXTRACTION EXPERIMENTS	42
4.3.1	Experiments with silt lens moisture content at 2.03% and 2.04%	42
4.3.2	Experiments with silt lens moisture content at 7.35% and 7.73%	43
4.3.3	Experiment with silt moisture content at 14.5%	44
4.4	MASS RECOVERY OF CARBON TETRACHLORIDE	45
4.5	MOISTURE CONTENT OF SILT LENS	46
4.6	INFLUENCE OF SILT MOISTURE	47
4.6.1	Zone 1	49
4.6.2	Zone 2	50
4.6.3	Zone 3	51
4.7	SUMMARY	53
5.0	CONCLUSIONS AND RECOMMENDATIONS	55
	BIBLIOGRAPHY.....	58
	APPENDIX A.....	62
	APPENDIX B	77
	APPENDIX C	81
	APPENDIX D.....	84

LIST OF TABLES

1.1 Liquid carbon tetrachloride inventory in the 200 West Area until FY 2008	7
3.1 Properties of silt	22
3.2 Conditions for the different experiments	26
3.3 Parameters for analysis method on the TCD (High and Low sensitivity)	33
3.4 Parameters for analysis method on the FID	33
3.5 Parameters for analysis method on the ECD	34
4.1 Mass of carbon tetrachloride recovered	46
4.2 Moisture content of silt particles.....	47
4.3 Summary of concentrations in each zone for all experiments	47
A.1 Data for 2.03 % moisture content experiment	63
A.2 Data for 2.04 % moisture content experiment	66
A.3 Data for 7.35 % moisture content experiment	68
A.4 Data for 7.73 % moisture content experiment	71
A.5 Data for 14.5 % moisture content experiment	73

LIST OF FIGURES

1.1 Various mechanisms responsible for contaminant transport in the subsurface	2
1.2 Hanford site map.....	4
2.1 Transport mechanisms for volatile organic compounds in the vadose zone	10
2.2 Schematic representation of competition between soil moisture and organic vapors for adsorption sites within the soil media.....	12
2.3 Conceptual model inter-particle transport	13
2.4 Schematic representations of mass transfer processes in the vadose zone	16
3.1 Schematic diagram of the 2-dimensional flow cell used for desorption studies.....	20
3.2 Schematic diagram of stainless steel mold and base plate for the silt lens.....	23
3.3 Schematic of the experimental layout showing the cell and GCs connected with valves, ‘T’ joints, and stainless steel lines	28
4.1 Typical concentration vs. time curve from a tracer test.....	38
4.2 Typical chromatogram obtained as GC response (analysis time=5 min).....	39
4.3 Typical concentration profile for desorption of carbon tetrachloride showing various zones	40
4.4 Concentration profiles for replicate runs. First run at 2.04 % moisture content and 305 mL/min. Second run at 2.03% moisture content and 315 mL/min	42
4.5 Concentration profiles for replicate runs. First run at 7.35 % moisture content and second run at 7.73% moisture content. Both experiments were conducted at flow rate of 309 mL/min	44
4.6 Concentration profile for single run at 14.5 % moisture content and 309 mL/min	45
4.7 Desorption profile for different moisture contents	49

4.8 Comparisons of normalized concentrations in Zone 1	50
4.9 Concentration profiles in Zone 2	51
4.10 Concentration profiles in Zone 3	52
D.1 Schematic of the ASE process	85

1.0 INTRODUCTION

There is widespread concern pertaining to the contamination of soils at the nuclear facilities in the country due to the release of a variety of contaminants into the environment resulting in subsurface contamination. Upon release these contaminants are either transported (migrate downstream or volatilize), transformed (physically, chemically and biologically) and/or accumulated on receiving media (adsorption). This contamination, although it occurred several decades ago, continues to violate existing regulatory limits (Poston et al., 2003). One such case is the presence of liquid carbon tetrachloride (CT) in the unsaturated (vadose) zone, at the Hanford Nuclear Reservation site in Richland, Washington. At Hanford, carbon tetrachloride was used as a carrier solvent for tributyl phosphate in the final purification of plutonium. It also served limited use as a thinning agent for machining of plutonium, after which it was discharged into unlined disposal trenches or cribs (Poston et al., 2003). Liquid wastes from the process were transported from the plutonium finishing plant to unlined trenches. The unlined trenches allowed carbon tetrachloride to migrate in to the vadose zone.

Although carbon tetrachloride is immiscible in water, it exhibits a relatively high solubility of 785 mg/L at 25 °C (O'Neil *et al.*, 2001). It also has a high degree of mobility in groundwater. Mobility above the water table can also occur through free product migration and vapor transport. There is hence widespread concern with regard to the effects of the carbon tetrachloride on human health. The regulatory standard for carbon tetrachloride is 5 μ g/L or 0.005 ppm in the aqueous phase (Poston et al., 2003).

Measurements made at several locations within Hanford have revealed a violation of the existing standards (Poston et al., 2003). Analysis of soil-gas samples from the subsurface

at Hanford has detected the presence of carbon tetrachloride vapors, which will ultimately escape into the atmosphere. Figure 1.1 describes the various mechanisms that contribute to the transport of volatile organic compounds (VOCs) from the source into the subsurface.

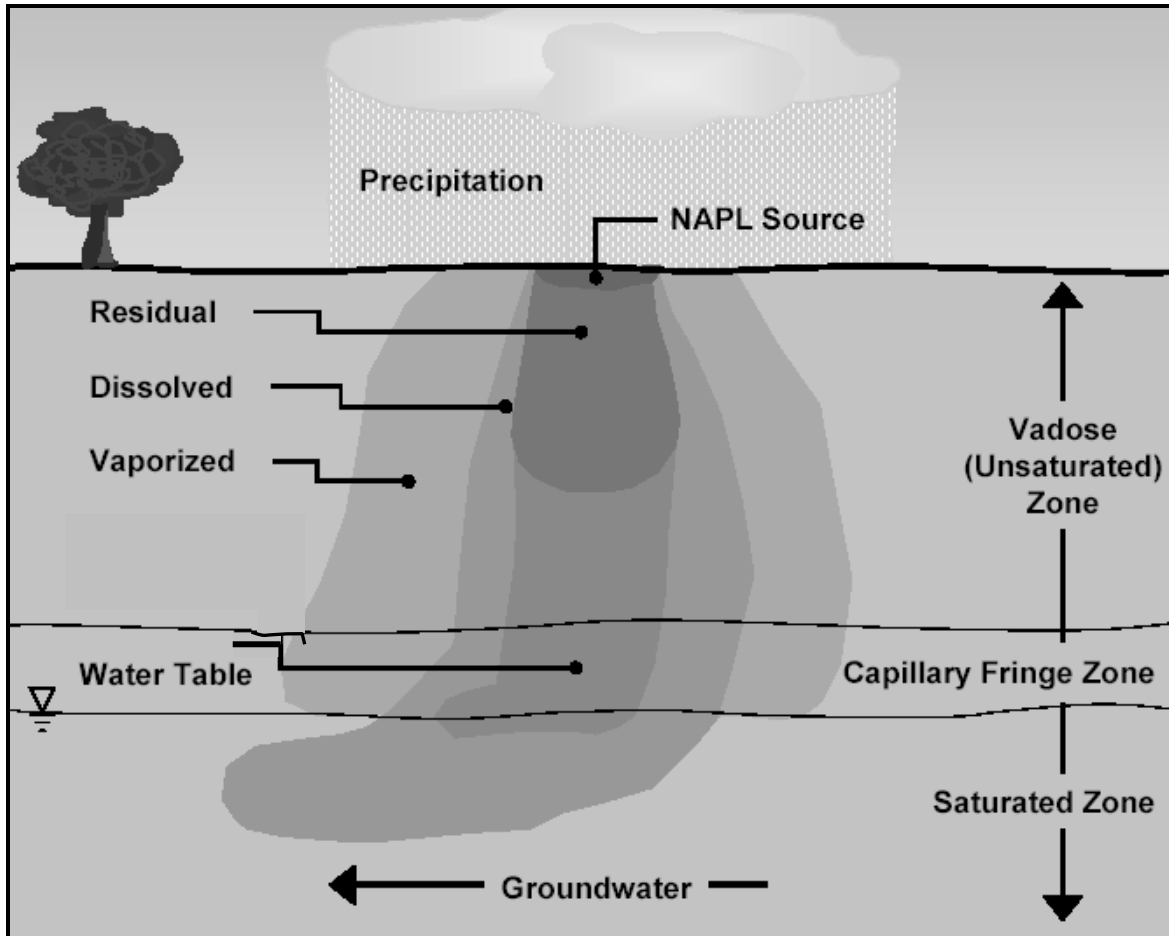


Figure 1.1 – Various mechanisms responsible for contaminant transport in the subsurface (Poston et al., 2003).

Efforts made towards cleaning the subsurface contaminants have resulted in the implementation of several remediation techniques. Primary among these are the pump and treat process for groundwater, and active and passive soil vapor extraction for VOCs in the subsurface. Soil-gas sampling techniques have also been used to monitor the movement of the contaminant vapors in the subsurface. This chapter presents an overview of the

problem concerning the contamination of carbon tetrachloride at the Hanford site. It includes characteristics of the site, details of the existing contamination, difficulties with the current theory and the objective of this study.

1.1 HANFORD SITE

The Hanford Nuclear Reservation is an approximately 586 square mile federal facility located in southeastern Washington, north of the city of Richland. The Columbia River flows eastward through the northern part of the site and then turns south, forming part of the eastern site boundary. The site was commissioned during World War II as part of the army's 'Manhattan Project' to produce plutonium for nuclear weapons (Poston *et al.*, 2003; Ward *et al.*, 2000; and Ward *et al.*, 2002). The 200 Area is situated centrally within the site and covers approximately 6 square miles. It is subdivided into the 200 East and 200 West areas. The 200 West Area covers approximately 5 square miles and is located south of the Columbia River while the 200 East Area which covers 7 square miles is west of the river. The maximum concentration of carbon tetrachloride under the 200 Area in the vadose zone has been measured in the 216-Z-1A tile field, the 216-Z-9 trenches and the 216-Z-18 disposal crib within the 200 West Area at Hanford with concentrations as high as 30,000 ppm being reported (Poston *et al.*, 2003; Ward *et al.*, 2000; and Ward *et al.*, 2002). Figure 1.2 shows the site map along with the various regions within the site.

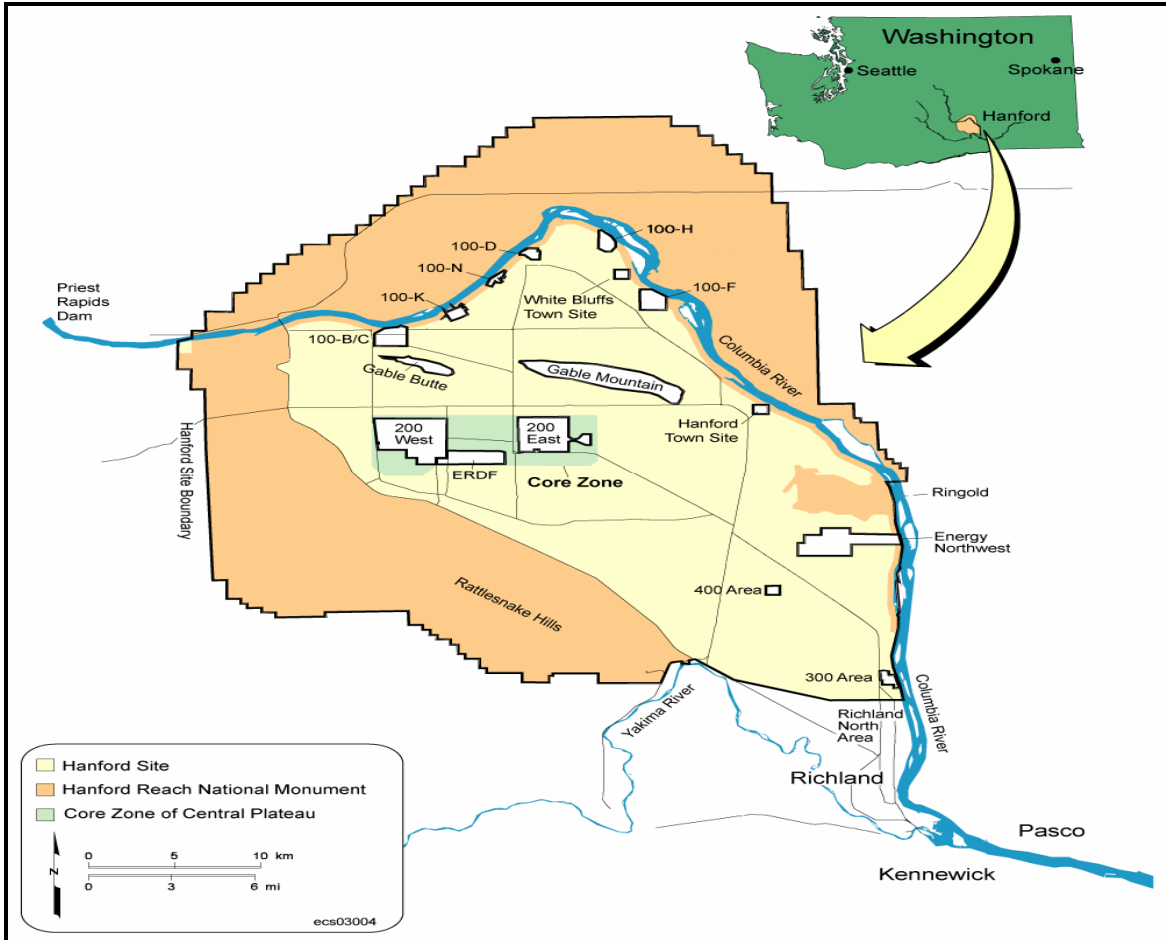


Figure 1.2 - Hanford site map (Poston *et al.*, 2003).

1.1.1 Site Characterization

The site is located in the Pasco Basin situated in the northern portion of the Columbian Plateau near the junction of the Yakima Fold Belt and the Palouse sub-provinces (Poston *et al.*, 2003; and Ward *et al.*, 2000). Catastrophic floods that occurred as a result of the breach of the glacial wall in western Montana and northern Idaho brought with them massive volumes of water across eastern central Washington. This process repeated itself numerous times about 13,000 years ago resulting in the formation of a thick sequence of sediments (gravel and sand). This formation, which is approximately 65 meters deep, comprises the uppermost layer (Poston *et al.*, 2003; and Ward *et al.*, 2000).

Layers of silt, gravel and sand (known as the ringold formation) form the middle level. This level extends almost 35-40 meters and is characterized by densely packed silt lenses (which exhibit low permeability) surrounded by sand and gravel. The middle level is confined below by a thick series of basalt flows that have been warped and folded, resulting in protrusions that crop out as rock ridges at certain locations. Both confined and unconfined aquifers can be found beneath the Hanford Site (Ward *et al.*, 2000; and Ward *et al.*, 2002).

In the 200 West Area, the uppermost aquifer is located in the ringold formation. It can be classified as an unconfined to locally confined or semi-confined aquifer. The depth of the groundwater table ranges from approximately 58 to 82 meters. In the area near the carbon tetrachloride disposal sites, the depth of the groundwater table is from 60 to 66 meters. The saturated thickness of the unconfined aquifer around the plutonium finishing plant is approximately 67 meters. It is laterally bound by the basalt ridges (which exhibit low permeability) and the Yakima & Columbia Rivers. These ridges act as a barrier to the lateral flow of groundwater when they rise above the water table (Ward *et al.*, 2000; and Ward *et al.*, 2002).

1.1.2 Contamination Inventory

All facilities located in the 200 West Area at Hanford produced nuclear fuel. Of the original carbon tetrachloride discharged in the 200 West Area, it has been estimated that approximately 21% was lost to the atmosphere by 1990, 2% dissolved in the upper 10 meters of the unconfined aquifer while the remainder made its way into the vadose zone and/ or groundwater where it resides in the vapor/ dissolved/ adsorbed phase and/or as dense nonaqueous phase liquid (DNAPL) (Poston *et al.*, 2003; and Ward *et al.*, 2000). It is

estimated that between 1955 and 1973, approximately 570,000 – 920,000 Kg of liquid carbon tetrachloride waste was discharged directly into trenches and cribs. It is also estimated that 119,700 to 196,800 Kg of carbon tetrachloride was lost to the atmosphere by direct volatilization. Assuming these estimates are correct 450,000 to 723,000 Kg of carbon tetrachloride remains in the subsurface.

The pump and treat process has so far removed 20,745 Kg from groundwater, active soil vapor extraction (SVE) has removed 173,300 lbs of carbon tetrachloride from the vadose zone & passive soil vapor extraction (PSVE) systems where natural pressure differences cause an air stream to flow through the existing SVE pipe network has cleaned up to 15,000 lbs of carbon tetrachloride (Poston *et al.*, 2003; Ward *et al.*, 2000; and Ward *et al.*, 2002). The remaining carbon tetrachloride is primarily concentrated in the vadose zone beneath the 200 West Area.

Pump and treat pilot scale operations commenced in 1992 and continued through 1996 when full-scale operations were initiated. The maximum concentration of carbon tetrachloride detected in groundwater when work started in 1990 was ~8700 μ g/L or 8.7 ppm while that measured in FY 2003 was 6900 μ g/L or 6.9 ppm (Poston *et al.*, 2003). SVE systems were operated at three different flow rates of 500 cfm, 100 cfm and 1500 cfm. The maximum vapor phase concentrations measured when work started in 1992 were in the range of 1,500 – 30,000 ppm. In FY 2003 the range was 97- 297 ppm. The system has removed 7% residual carbon tetrachloride from the 216-Z-1A tile field & 216-Z-18 crib and 22% residual carbon tetrachloride from the 216-Z-9 trench. In 2003 all wells were operated at 500 cfm only (Poston *et al.*, 2003). Table 1.1 provides a summary of the carbon tetrachloride cleanup in the 200 West Area at Hanford.

Table 1.1 - Liquid carbon tetrachloride inventory in the 200 West Area.

Location	Total Contamination (Kg)	Total volume treated (Million liters)	Total mass removed (Kg)	% Removal
Groundwater Plume	570,000 to 920,000	1,950	7,668	2%
Vadose Zone		-	79,164	17%

1.2 DIFFICULTIES WITH THE CURRENT THEORY

The present inventory of contaminants at the site clearly shows only an estimated 17-19 % of carbon tetrachloride that has been removed. A significant portion of the carbon tetrachloride is firmly bound to the soil particles and is difficult to remove. The results from field tests do not show the higher level of removal efficiency that has been achieved in laboratory studies. Spatial and temporal variations encountered at sites are the primary reasons for this failure (Hughes *et al.*, 1992; McClellan *et al.*, 1992). It has been observed during cleanup and in studies conducted in the laboratory that the desorption profile (vapor phase concentration) is characterized by high initial concentrations followed by a slow tailing phenomenon (at low concentrations) extending over several months (McClellan *et al.*, 1992; and Pavlostathis *et al.*, 1992).

This slow release can be attributed to a variety of processes like inter and intra particle diffusion and slow desorption causing a delayed vapor transport as the contaminant slowly partitions into the vapor phase. Mathematical models have been used extensively to study and predict the fate and transport of carbon tetrachloride. These models are prepared under a variety of assumptions to suit the requirements of the site and

are validated using laboratory and field data. These models have however failed to predict the desorption behavior exhibited during pilot and full scale operations (Stephens *et al.*, 2000).

1.3 OBJECTIVE

It is known that the presence of water sets up a competition between water and carbon tetrachloride for adsorption sites affecting the adsorption of carbon tetrachloride onto the soil and can effect desorption rates by impacting boundary layer diffusion (Nyer *et al.*, 1996). This thesis investigated the effect of moisture content on desorption of carbon tetrachloride from Hanford silt in a simulated vadose zone environment. Experiments were conducted at a constant flow rate and initial carbon tetrachloride concentration in a two-dimensional stainless steel extraction cell. The vadose zone profile was simulated in the lab by embedding a silt lens within a layer of sand through which air was passed at a constant flow. The moisture content of the silt was varied over a range typical for the Hanford site. During each experiment flow cell effluent concentrations were monitored as a function of time.

2.0 LITERATURE REVIEW

In the subsurface a NAPL may partition into various phases after it is initially introduced as a liquid. A portion will remain in the liquid phase as residual, but the rest may partition into the pore water, adsorb to soil organic matter and particles, or partition into the vapor phase. The concentration in each of these phases will depend upon properties of the soil (organic matter content and water content), that of the contaminant (solubility, vapor pressure, and partitioning coefficients), and system conditions (temperature, barometric pressure, flow rate and the duration of time since the introduction of the pure phase) (McClellan *et al.*, 1991). Theoretically, given enough time and appropriate system conditions, equilibrium may be achieved amongst all these phases. Equilibrium between the various phases can be achieved in a controlled environment within a laboratory. However site conditions are never ideal and as a result complete equilibrium is difficult to achieve (McClellan *et al.*, 1992, and Benson *et al.*, 1992).

The vapor phase concentration of any gas in air can be expressed by the following equation:

$$C_v = \frac{1 \text{ volume of gas pollutant}}{10^6 \text{ volumes of air}} = \text{ppm} \quad (2.1)$$

Where

C_v = vapor phase concentration, ppm;

When a NAPL plume is introduced in to the vadose zone, it will initially undergo volatilization. However some portion will continue to remain as a NAPL. The vapor, resulting from the volatilization, will adsorb on to available sites on and within the soil

particles, some will partition into the water associated with the soil (boundary layer and intraparticle water) while another portion will dissolve into the groundwater (interparticle water). Some of the vapor will make its way out of the soil and will be released in to the atmosphere. Figure 2.1 shows the various contaminant pathways within a typical vadose zone/groundwater soil system.

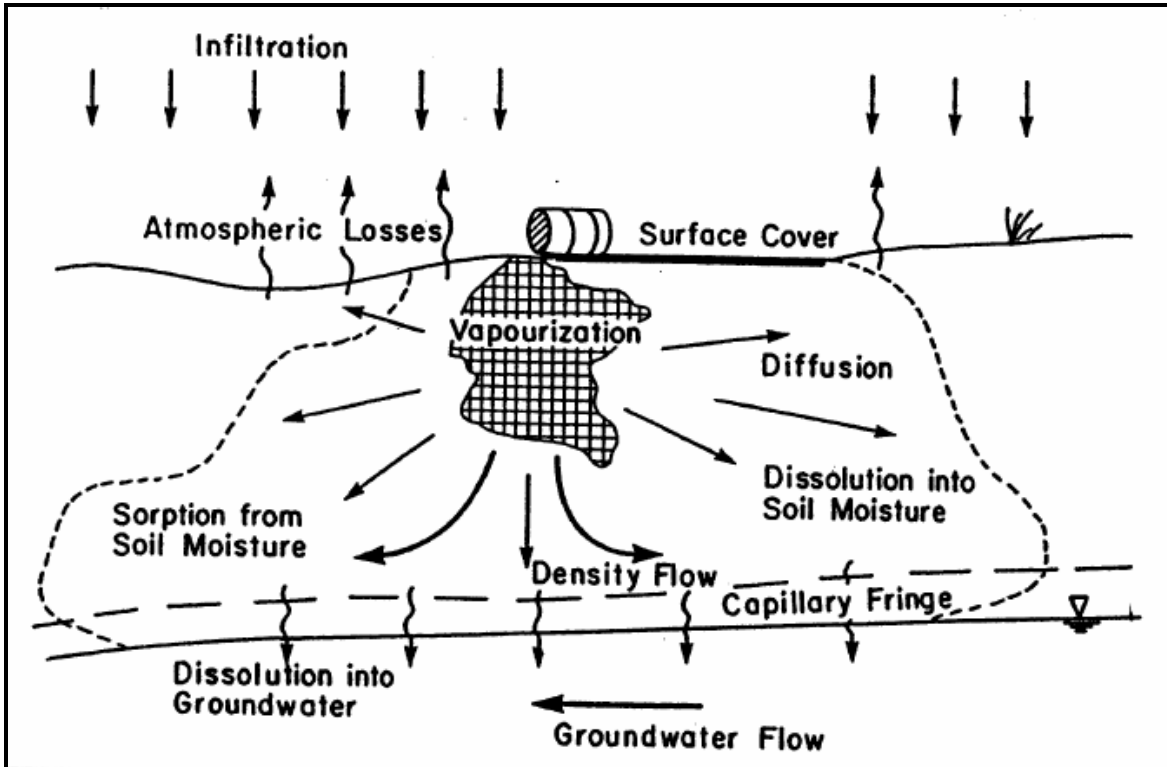


Figure 2.1 - Transport mechanisms for Volatile organic compounds in the vadose zone (Mendoza *et al.*, 1990).

The main modes of transport of contaminants in the subsurface are advection (function of fluid flow) and dispersion. Dispersion can be either mechanical dispersion (where contaminants traveling at different velocities mix) or molecular diffusion (where contaminants travel from a region of higher concentration to lower concentration).

2.1 LABORATORY STUDIES

Various investigative studies have been undertaken relating to equilibrium criteria for volatile organic vapor transport. These range from validation of the equilibrium assumptions for vapor transport (Cho *et al.*, 1990), rate limited desorption noticed as extended tailing during venting operations (Bloes *et al.*, 1992), ability of the contaminant to spread at the water-gas interface in moist field conditions (Wilson *et al.*, 1992), effect of flow rate, spill size and configuration, soil properties and boundary conditions (Benson *et al.*, 1992; and Ford, 1996). These case studies have provided valuable insight in understanding the equilibrium conditions and processes governing the cleanup of carbon tetrachloride from the simulated vadose zone box system in this thesis. The following subsections discuss the effect of soil moisture, soil structure, the various forces that facilitate transport and hysteresis on contaminant removal.

2.1.1 Effects of Soil Moisture

When introduced in the soil medium, water molecules form a monolayer around and within soil particles, hydrating all available surfaces before aggregating in multilayers. At increased water content, soil moisture content increases primarily by pore condensation. Capillary conditions restrict solvent vapor access to interior surfaces for adsorption, fewer mineral sites are available and at some point surfaces are covered with sufficient water to negate direct surface interactions. Water molecules were seen to aggregate at surface sites with high excess surface energy, denying availability to solvent molecules and reducing weakly polar (organic) phase sorption (Tekrony *et al.*, 2001). Figure 2.2 gives a schematic representation of the effect of soil moisture on the adsorption of VOCs.

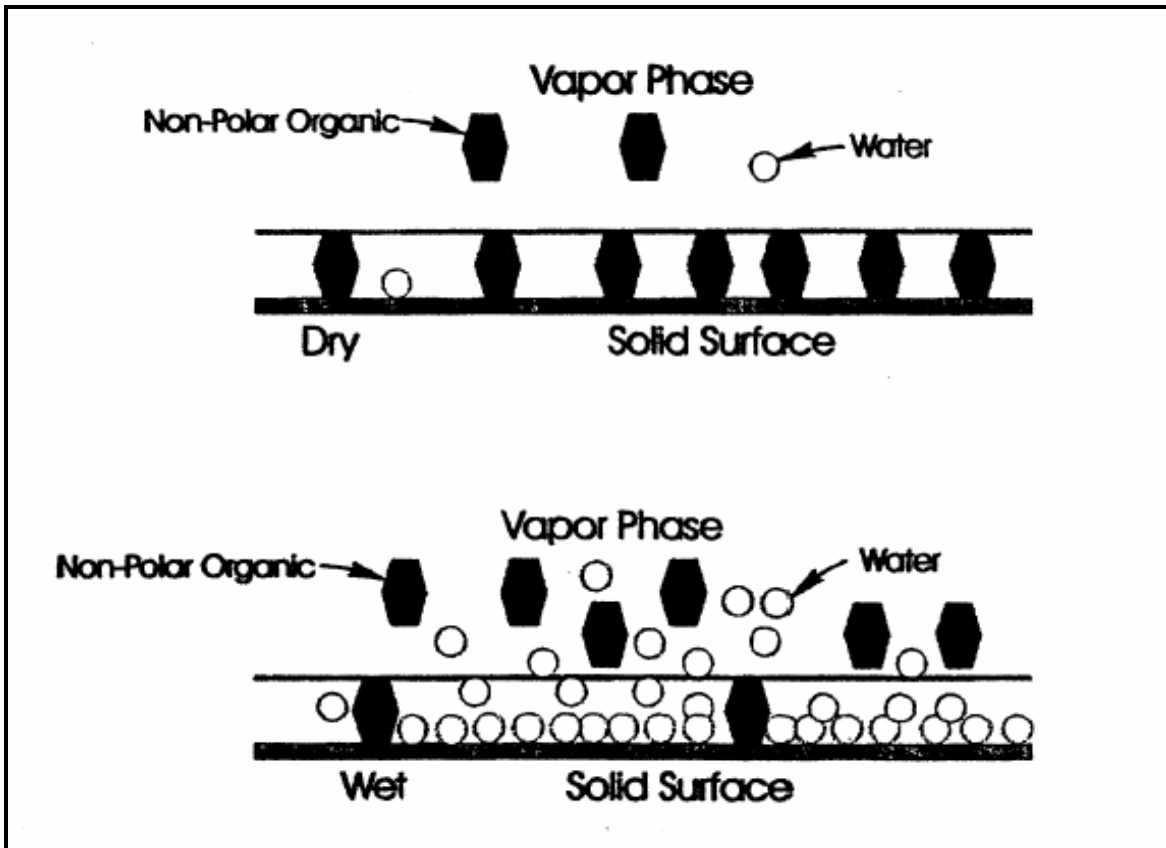


Figure 2.2 - Schematic representation of competition between soil moisture and organic vapors for adsorption sites within the soil media (Nyer *et al*, 1996).

Tekrony *et al.* (2001) showed evidence that adsorption of VOC vapors on sandy loam was greatly decreased with an increase in moisture content. They observed that at water content greater than 0 %, dissolution into the bound water and adsorption at gas interface compete with direct adsorption of solvent onto the soil. Hughes *et al.*, (1992) concluded that the high organic carbon and moisture content result in greater vapor retardation capacity and the high moisture content provides a greater barrier to diffusion at lower concentrations. Organic contaminant adsorption in presence of water occurs through one of the following processes:

- Adsorption onto the mineral surfaces through the gas phase (gas-solid interface).

- Adsorption onto the mineral surface through the adsorbed water phase (liquid-solid interface).
- Adsorption onto the surface of an adsorbed water film (gas-liquid interface).
- Dissolution into adsorbed water.
- Dissolution into organic matter through the adsorbed water phase.
- Dissolution into organic matter from gas phase (Thibaud *et al.*, 1993).

2.1.2 Effect of Soil Structure

Inter-particle interactions

Wilkins *et al.* (1995) conducted one dimensional column experiments to investigate the mass transfer limitations associated with volatile organic vapor transport and its equilibrium. They hypothesized that the distribution of entrapped NAPL within water saturated porous media consists of both individual NAPL globules in single pore bodies and larger branched ganglia including several pore bodies and interconnected pore throats. Figure 2.3 shows this conceptual model structure.

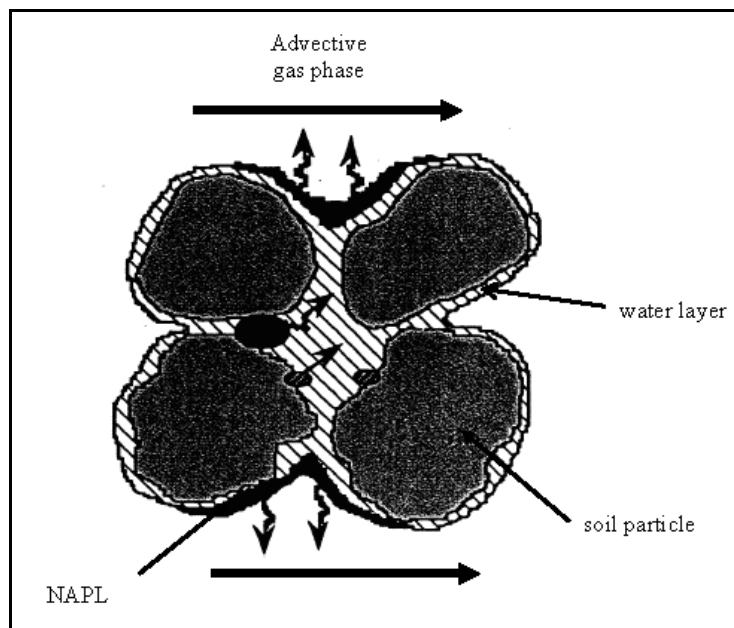


Figure 2.3 - Conceptual model describing inter-particle transport (Wilkins *et al.*, 1995).

The NAPL thus exists as thin films between the residual water phase, which preferentially occupies the smaller pores, and the gas phase, which continuously fills the larger pores. The mean grain size also has a significant control on the fluid phase saturation and interphase mass transfer. The residual saturation consists of continuous films, pendular rings, wedges surrounding aqueous pendular rings, and filled pore throats. A portion of the residual NAPL may be isolated within pore throats or between aqueous phase wedges. In the presence of water, a decrease in soil grain size was seen to produce smaller, more spherical entrapped NAPL globules (Wilkins *et al.*, 1995). This reduces the availability of the entrapped NAPL to the mobile gas phase and mass transfer may become rate limited by diffusion through zones of immobile water (Wilkins *et al.*, 1995).

Intra-particle interactions

Pores within the soil particles (intraparticle) can be classified according to their internal diameters as follows:

- Micropores (dia < 20 $\overset{\circ}{\text{A}}$).
- Mesopores (20 $\overset{\circ}{\text{A}}$ < dia > 500 $\overset{\circ}{\text{A}}$).
- Macropores (> 500 $\overset{\circ}{\text{A}}$) (Baklanov *et al.*, 2000; Ford, 1996).

Farell *et al.* (1994b) studied the effects of capillary forces on the pore structure of model solids, aquifer materials, and soils. They deduced that capillary condensation which is the liquification of a gas in a near-molecular size space at higher temperature and lower vapor pressure than otherwise would occur is associated with mesoporosity. They also deduced that solids possessing only macroporosity show little or no capillary effects. Molecules adsorbed in micropores are subject to stronger field strengths than those adsorbed on flat surfaces. For cylindrical pores 5 adsorbate diameters or less in size, adsorption energies

increased with decreasing pore size. Pores 3 adsorbate diameters or less were found to possess significant increased interaction potentials and as pore size approached that of the adsorbate, interaction potentials were calculated to become more than five times those on flat surfaces. Thus pores with diameter $\sim 20 \text{ \AA}$ or less (for carbon tetrachloride molecular diameter is $\sim 5 \text{ \AA}$) were expected to have increased adsorption energies and increased capacities of sorption.

2.1.3 Various Forces that Facilitate Transport

There are several forces that influence a contaminant as it migrates within the vadose zone. These are:

- Capillary forces (interparticle capillaries).
- Viscous forces.
- Gravity/ buoyant forces (Wilkins *et al.*, 1995).

Of these the capillary forces are the most dominant in moist conditions. The capillarity is a function of the cohesive forces within each liquid (both contaminant and soil moisture) and the adhesive forces between the liquid and solid phase in the system. Carbon tetrachloride has a tendency to exhibit low interfacial tendencies with water and gas phases and coalesces into lenses within the interparticle pore spaces (Wilkins *et al.*, 1995). These lenses are separated by thin films of soil moisture, leading to their unavailability for mass transfer (Wilson *et al.*, 1992). Once residual saturation of the contaminant is attained, transport can occur only in gaseous and aqueous phases. In the case of highly volatile organic solvents that exist preferentially in the gaseous phase, vaporization at the source will produce a saturated gas mixture, and transport will be primarily by gaseous phase advection and dispersion (Mendoza *et al.*, 1990). Since the gas mixture will be in continuous contact with the soil moisture, organic mass will be transformed to the water

and soil solids by phase partitioning. When the organic vapor has spread, partitioning between the gaseous phases will lead to contamination of the soil moisture (Mendoza *et al.*, 1990). Figure 2.4 describes the various mechanisms of mass transfer

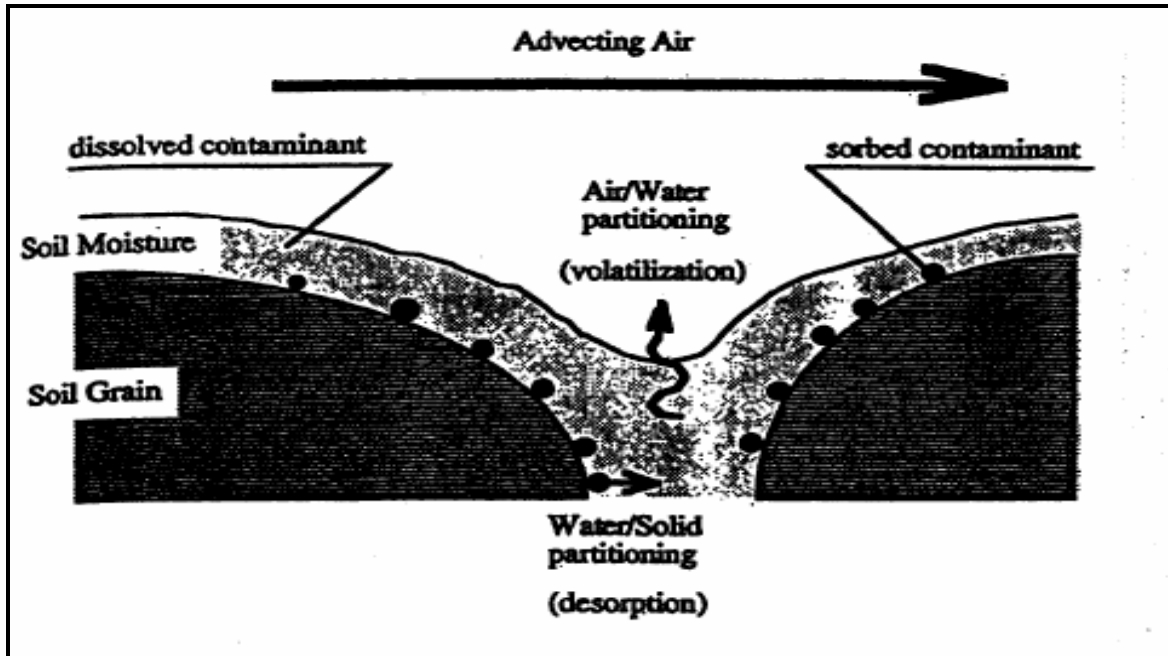


Figure 2.4 - Schematic representations of mass transfer processes in the vadose zone (Armstrong *et al.*, 1994).

During cleanup, after the pure phase is removed, a small but environmentally significant mass of original contaminant may still remain in the soil. McClellan *et al.* (1992) conducted field SVE experiments to study the cleanup of trichloroethylene (TCE) in the vadose zone at the Borden site in Canada. Their work showed that SVE was less effective for removal of TCE in the aqueous and adsorbed phases. Relative removal efficiencies were high during pure phase removal but the rates declined sharply as the pure phase was depleted and the rate of removal seemed to be controlled by the kinetics of mass transfer from the adsorbed to the dissolved to the gas phase. The removal efficiency declined to very low values as the concentration in both the dissolved and adsorbed phase approached environmentally acceptable values.

The removal of organic phase (free product) TCE was advection dominant while the removal of dissolved and adsorbed phases was limited by non-equilibrium mechanisms like mass transfer, rate-limited desorption, and/or diffusion from immobile zones (McClellan *et al.*, 1992). Falta *et al.* (1993) observed that in the absence of residual NAPL, the effect of diffusion was much smaller and that the rate of contaminant removal was primarily by the rate of gas flow through the contaminated region. In the case where the VOC was strongly partitioned into the aqueous and solid phases, the rate of local interphase mass transfer into the gas phase was seen to also limit the rate of contaminant removal. Brusseau *et al.* (1997) grouped rate-limiting processes into two general classes: transport related and sorption related. Transport-related non-equilibrium, often referred to as physical non-equilibrium, results from existence of a heterogeneous flow domain. Sorption related non-equilibrium might result from chemical non-equilibrium or from rate-limited diffusive mass transfer. They found that non-equilibrium was caused by rate-limited interactions between the sorbate and sorbent. They suggested three different mechanisms could cause sorption related non-equilibrium:

- Film diffusion.
- Retarded intraparticle diffusion.
- Intrasorbent diffusion.

2.1.4 Effect of Hysteresis

The adsorption/desorption process is often simplified by assuming ideal conditions of instantaneous equilibrium, isotherm linearity and complete desorption reversibility. However adsorption and desorption equilibria are often not the same. This phenomenon known as hysteresis is one where a significant deviation of the desorption curve from the adsorption curve is observed (Patakioutas *et al.*, 2002; Chen *et al.*, 2000; Farrell *et al.* 1994;

Konstantinou *et al.*, 2000; and Pavlostathis *et al.*, 1991). Kan *et al.* (1994) showed that a pollutant could be irreversibly bound without chemically reacting with the soil matrix, if some physical alteration of the soil takes place. The irreversibly adsorbed fraction is of significant interest and uncertainty, because it affects chemical fate, toxicity, risk to human and aquatic life and the efficiency of most remediation technologies.

Yonge *et al.* (1985) showed that the degree of irreversibility was as high as 85-97% for certain phenolic compounds. Lab studies on sediments with varying particle size and organic carbon content showed that desorption deviated significantly from the adsorption (Chen *et al.*, 2000). Several explanations have been provided for hysteresis. Patakioutas *et al* (2002) and Pavlostathis *et al* (1991) showed that hysteresis is more pronounced for soils with higher organic matter content. They claim that the organic matter fraction of the soil is responsible for the presence of hysteresis, a claim supported by Konstantinou *et al* (2000). Yonge *et al.* (1985) postulated high energy bonding (chemisorption) to be the cause of strong irreversibility. They concluded that irreversibility was found to be a function of initial soil phase concentration, soil organic carbon and residence time. Kan *et al.* (1994) conducted experiments in batch reactors (vials) and studied the effect of hysteresis on desorption of organic vapors. They provide the following reasons for hysteresis:

- Varying adsorption energies leading to isotherm non-linearity.
- Failure to attain equilibrium in either adsorption/desorption direction due to the slow kinetics in either step.
- Chemisorption of the pollutant to various components of the soil matrix, causing irreversible adsorption.
- Biotic/ abiotic degradation, causing irreversible adsorption.
- Capillary condensation.

2.2 SUMMARY

Desorption occurs in two phases, initial desorption from the multi-layers followed by desorption from the mono-layers. The contaminant will occupy the smaller pores within the soil structure and will not be readily available for desorption thus delaying the cleanup process. When the contaminant is present in the pure phase, it enters the groundwater via dissolution of volatilized vapors into soil moisture. However for the adsorbed or aqueous phases diffusion is more dominant as compared to advection for partitioning. Under “wet” conditions, capillary forces acting within the system are responsible for the separation of organic contaminant molecules as distinct globules separated by thin films of water, increasing their availability for partitioning or removal. If the internal pore structure undergoes changes during the adsorption process due to the presence of water this may cause a delay or lag in the desorption process as the contaminant may not be available for removal.

3.0 EXPERIMENTAL METHODS

3.1 VACUUM EXTRACTION CELL

3.1.1 Design

A stainless steel cell with dimensions of 2.44m x 0.61m x 0.152m (Ford, 1996) was used to perform the vapor extraction experiments. A schematic diagram of the cell is presented in Figure 3.1.

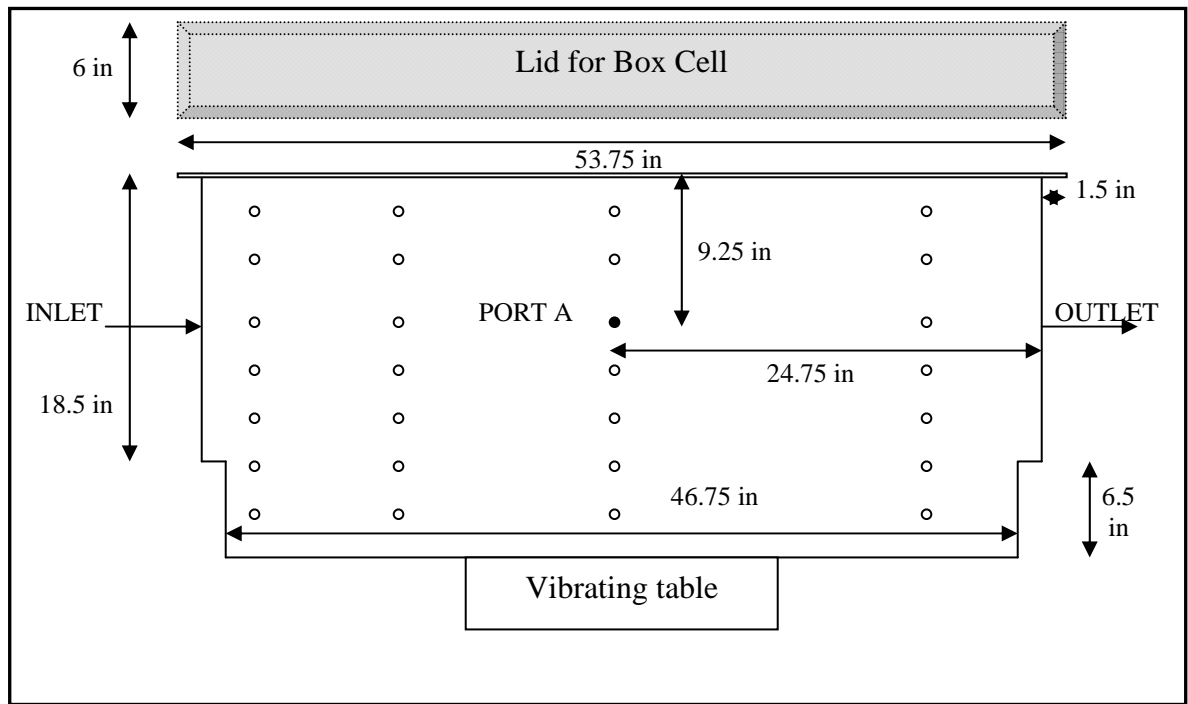


Figure 3.1 – Schematic diagram of the 2-dimensional flow cell used for desorption studies.

The cell consists of 3 mm thick stainless steel plates. Stainless steel angle iron was welded along the top perimeter of the cell to create a lip 2.5 cm wide in which 24 holes were drilled equidistant (12.5 cm apart from each other) along the perimeter to receive a 3 mm stainless steel lid that was fastened using 2.5 cm bolts. A shallow channel was provided around the perimeter of the cell by placing 3 mm stainless steel strips between the lip and the cell lid. A 6 mm viton o-ring (ERIKS West Inc., Fluoroc-75) gasket was

placed in the channel to create an airtight seal. Silicone sealant (GE Adhesives, Grade II transparent) was used to hold the o-ring, the strips and the lid in place and finally 2.5 cm stainless steel bolts were used to hold the lid down.

At both ends of the cell, holes were tapped 0.23 m from the top to serve as the inlet and the outlet ports. There were 28 sampling ports, 10 mm (1/4 in) wide installed on the front face of the cell, which were capped with 10 mm (1/4 in) stainless steel nuts (with Teflon septa) and sealed. These ports were used earlier for experiments conducted by Ford (1996). In this research, the ports were used to check for vacuum in the box when it was tested for leaks. The box was placed on a vibrator table (FMC Syntron Vibrating Table, Model VP51D1). Two vertical 'U' braces were used with steel plates and bolts to laterally support the cell. These prevented the cell walls from bulging outward from the weight of the sand.

A piece of centered stainless steel plate was placed 25.4 mm (1 inch) from each end of the cell. The gap formed was filled with 0.2 mm diameter glass beads (E. R. Advanced Ceramics, Inc., East Palestine, OH). The glass beads along with the centered plate provided uniform flow through the cell minimizing channeling. After the cell setup for each experiment was completed and subsequently sealed, a 24- hour period was provided for the sealant to cure. Successive to this a leak check was performed to ensure that the system was airtight. For this the inlet and the injection port, and other sampling ports were capped, while a vacuum pump (Metal Bellows Inc, Model MB-21) was attached to the outlet end of the cell. The pump was started and the system was subjected to a vacuum of about 40.0 cm water. The pump was stopped and measurements were

taken every two hours to check for changes in vacuum. A drop of 5.0 to 7.5 cm water over a period of 2 hours was considered allowable.

3.1.2 Setup and Operation

The media used for all experiments was commercially available silica sand (US Silica, F-35 grade) and uncontaminated silt (Table 3.1 below lists properties of silt) from the Hanford Site (200 West Area).

Table 3.1 – Properties of silt

Description	Organic Carbon (%)	Organic Matter (%)	CEC Cmol (+)/Kg	Grain Size
Hanford silty sand	0.22	0.38	9.1	P ₁₀ = 0.015 mm P ₆₀ = 0.090 mm
Notes				
CEC - Cation Exchange capacity				
Hanford silt has a porosity of 0.5				

sieve analysis

Diameter of the sieve (mm)	% wt finer than
0	0
0.075	~80
0.15	~85
0.425	~98
0.85	100
1.75	100
4.75	100

The sand simulated the uppermost layer (of the vadose zone) at Hanford, while the silt simulated the low permeability regions within the vadose zone at Hanford. The sand was added to the cell in layers of approximately 5 cm and gently vibrated for 10 seconds using a plate vibrator (FMC Syntron Vibrating Table, Model VP51D1). It was important to minimize use of the vibrator to a few seconds in order to prevent excessive compaction.

When the sand layer reached 2.5cm below the level of port 'A' (marked in Figure 4.1), the silt lens was introduced. The main factor in all experiments was the moisture content of the silt lens. The procedure for either verifying or increasing the moisture content of the silt lens is provided in subsequent sections. The silt lens was prepared externally using a mold of internal dimensions of 10cm x 20 cm x 10 cm made from 2 mm stainless steel plates. The mold was provided with 'U' hooks welded to all four corners. A 6 mm thick base plate (12.5 cm x 25 cm) with similar 'U' hooks was used. The mold was held in place on the base plate using rubber bands. The mold and the base plate were then weighed before introducing the silt. Figure 3.2 provides a schematic of the mold apparatus.

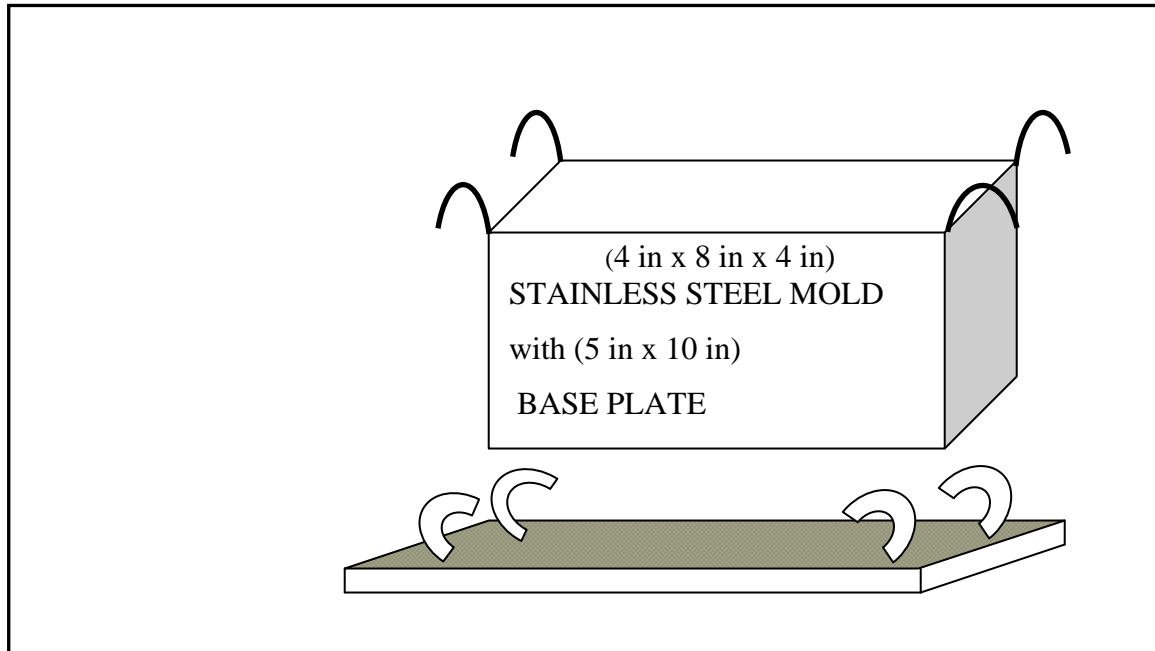


Figure 3.2 – Schematic diagram of stainless steel mold and base plate for the silt lens.

Uncontaminated Hanford silt was passed through a No. 18 sieve (ASTM Specification, 1mm mesh opening size). Samples were collected for moisture content determination of the silt as explained in section 3.4.1. The silt was added to the mold up to

the 5 cm mark. The silt layer thus formed was compacted using the standard procedure for compaction (Bailey *et al.*, 2003). A 2.5 Kg compaction hammer was dropped 25 times from a height of 0.33 m. This procedure was repeated over the entire silt layer. An additional 5 cm was added and the compaction procedure was repeated until a silt lens of 10cm x 20 cm x 10 cm was ready. The silt lens along with the mold and base plate were then weighed.

Four clamps were fixed on the lip edge of the cell above the port A (Figure 4.1). The mold with the lens was lowered into the cell and placed on the sand layer, approximately 5 cm below port 'A'. The center of the mold was aligned with the center of the port 'A'. Twine was attached to each of the four hooks on the mold and then entwined around the four clamps at the lip of the cell. The rubber bands were cut and the base plate was slowly slid from under the mold. Sand was added again in layers until it was level with the top of the mold. The mold was raised from the sand using the twine without disturbing the silt lens. The sand around the lens provided support and prevented it from collapsing. The silt lens was thus firmly centered and embedded in the sand.

After the mold was removed, sand was added again in layers as before and vibrated for 10 seconds for each layer. When the sand reached the angled lip at the top of the cell, it was leveled using a straight edge. Using a brush with stainless steel hair, sand was carefully removed from the crevices formed by the welds that run along the perimeter of the lip. The entire lip edge of the cell was then vacuumed (Shop-Vac Co., model QSPRO - 12 gallons) to remove any sand particles that may have been left behind. It was important to clear all sand particles that could compromise the integrity of the seal on the cell.

Silicone sealant was applied along the periphery of the box on the angled lip. The 2.5 cm wide side plate was firmly pressed into place. The sealant is cleared from the holes provided for the bolts. The o-ring measured to exact length was then set into the channel using sealant. Finally the stainless steel lid is glued into place with sealant and then bolted down using 24 stainless steel bolts with double washers and hex nuts.

The inlet and outlet ports consisted of 5 mm (1/8 in) pipe fitting that was inserted into a tapped hole drilled on the side plate of the cell. The vacuum pump was then started. A four-channel Tylan flow control unit (Tylan Inc, Model RO-28) and a mass flow controller (Kalrez Mass flow controller, Model FC-260 KZ) preceded the pump and were used to maintain a flow rate between 300 and 310 mL/min. A soap film meter (Hewlett Packard, model 0101-0113) was used to calibrate the mass flow controller and as a secondary means of checking flow. The Tylan had to be adjusted each day to maintain the desired flow rate through the cell. The flow exiting out of the system was also checked to ensure there were no losses in the flow cell system.

3.2 TEST RUN CONDITIONS

This section describes the different experimental conditions used to determine the effects of silt moisture content on the desorption profile. The conditions are listed in the Table 3.2. The initial moisture content of the sand was fairly similar for all experiments and was always <0.1%.

Table 3.2 - Conditions for the different experiments.

Run #	Conditions for the run
Run 1	<ul style="list-style-type: none">- 55 mL of carbon tetrachloride injected into the center of the silt lens.- Silt lens at residual moisture content of 2.03%.- Flow and sampling commenced at least 24 hours after injection.
Run 2	<ul style="list-style-type: none">- Repeat of the above run.- 50 mL of carbon tetrachloride injected into existing silt lens.- Flow and sampling commenced at least 24 hours after injection.
Run 3	<ul style="list-style-type: none">- Fresh silt lens was added for this run.- 52 mL of carbon tetrachloride injected into the center of the silt lens.- Moisture content of the silt lens 14.5%.- Flow and sampling commenced at least 24 hours after injection.
Run 4	<ul style="list-style-type: none">- Fresh silt lens was added for this run with moisture content at 7.35%.- 50 mL of carbon tetrachloride injected into the center of the silt lens.- Sampling commenced at least 24 hours after injection.
Run 5	<ul style="list-style-type: none">- Fresh silt lens was added for this run with moisture content at 7.73%.- 50 mL of carbon tetrachloride injected into the center of the silt lens.- Flow and sampling commenced at least 24 hours after injection.

3.2.1 Flow rate, Temperature, and Relative Humidity

A flow rate of 309 mL/min was maintained within the system at all times. The flow rate was checked every hour (for the first 6 hours), then every 3 hours (for the next 12 hours) and subsequently every time a sample was taken. The temperature and relative humidity of the air in the room were recorded to observe any untoward fluctuations. A digital humidity and temperature gauge (Accurite Co.) was used for this purpose. The room temperature ranged between 20 and 30 °C, and the relative humidity varied between 20 and 30 %.

3.3 SAMPLING PROCEDURE

All stainless steel fittings were purchased from Swagelok Co., Ohio, U.S.A. All the stainless steel lines were purchased from Alltech Associates Inc., Illinois, U.S.A, and the Teflon septa from Supelco Company, Pennsylvania, U.S.A. The liquid carbon

tetrachloride injection port on the cell consisted of a 10 mm (1/4 in) tube fitting inserted into a tapped hole drilled on the front face of the box, which could receive a 10 mm (1/4 in) stainless steel nut. A Teflon septum was used with the nut to provide an airtight seal. While injecting the liquid carbon tetrachloride, the needle was passed through the septum into the silt lens.

The liquid carbon tetrachloride (Aldrich Chemical Co. Inc., 99% purity) was introduced into the silt lens at the rate of 1 mL/min. A syringe pump (KD Scientific, model 210) was used with a 60 mL plastic syringe (Monoject Co.) and a 15 cm long stainless steel needle special ordered from Hamilton Co. (model N722). The syringe pump was carefully aligned at the level of port 'A' (Figure 3.1), so as to pass through the septum, penetrate the sand layer and reach the center of the silt lens. The septum was checked for visible signs of rupture due to the insertion of the needle. If cracks were found the septum was sealed with silicone sealant. Flow and sampling were commenced 24 hours after injection.

In preliminary trials vapor samples from the cell were injected into the gas chromatograph using 20 mL plastic syringes (Monoject Co.). A luer lock tip sampling port was connected to the outlet end of the vacuum pump. Samples were drawn at the rate of ~300 mL/min into syringes which were then immediately capped. The sample from the syringe was then injected into the chromatograph. The sample was held in the syringe for approximately 1 min before injection. Data however showed that a considerable amount of carbon tetrachloride was being lost through sorption into the plastic syringe body. This sampling technique was discontinued. The new sampling technique included using

stainless steel lines that ran from the experimental cell directly to the gas chromatographs.

A schematic of the experimental layout is provided in Figure 3.3.

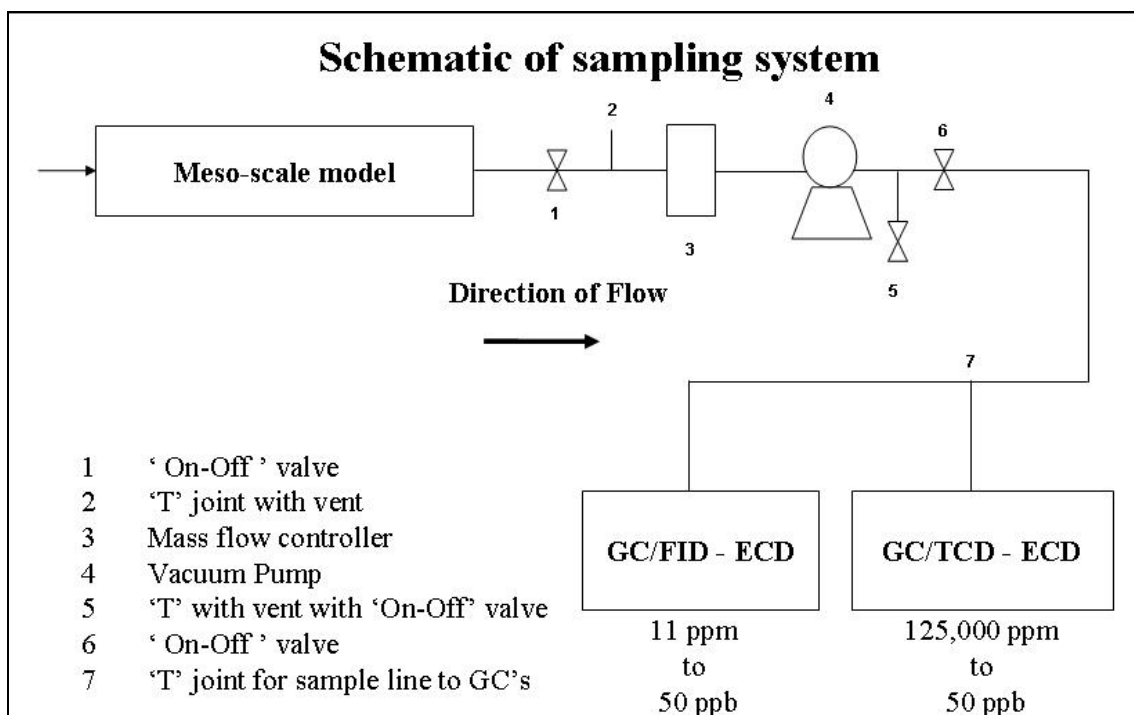


Figure 3.3 – Schematic of the experimental layout showing the cell and GCs connected with valves, ‘T’ joints, and stainless steel lines.

The outlet port of the cell was connected to a stainless steel valve with 5 mm (1/8 in) stainless steel tubing. The valve led to a ‘T’ connection which had one end ending in an exhaust vent that could be shut off with a stainless steel nut. The other end of the ‘T’ was connected to the inlet of a vacuum pump via a 5 mm (1/8 in) fitting.

The outlet of the vacuum pump was connected to another ‘T’ connection with 5 mm (1/8 in) stainless steel tubing. The ‘T’ connection consisted of an exhaust vent (that could be shut off with a 5 mm (1/8 in) stainless steel cap) and 5 mm (1/8 in) stainless steel tubing that was connected to another valve. Finally ~20 feet of 5 mm (1/8 in) tubing connected the valve to the gas chromatograph, which was in an adjoining laboratory. The

residence time in the line from the cell to the instrument was measured to be less than 3 seconds.

3.4 MOISTURE CONTENT OF SILT LENS

3.4.1 Measuring Residual Moisture Content

The uncontaminated silt obtained from the Hanford site was stored in 5 gallon plastic buckets (Norpack Inc) with airtight lids. To measure the moisture content of the silt, triplicate samples (~10g each) were taken from the bucket and weighed in aluminum dishes. The weight of the aluminum dishes was recorded first. The samples with the aluminum dishes were then placed in an oven (Blue M Electric Co., Stabil-Therm gravity oven) at 105 °C overnight to allow the residual water to evaporate. The dishes were then placed in a desiccator (Sanplatec Corp.), containing calcium sulfate as the desiccant (W.A.Hammond Drierite Ltd., size 8 mesh pellets) and humidity controller. The dishes were finally weighed after they had attained room temperature (after ~ 4 hours). The moisture content was calculated using the following relation (Holtz *et al.*, 1981):

$$\text{M.C.} = (W_w/W_s) \times 100 \quad (3.1)$$

Where

W_s = weight of dry soil, g;

W_w = weight of water, g; and

M.C. = moisture content, %.

The moisture content of Hanford silt was measured to be ~2% while that of the sand purchased commercially was found to be <0.1%. The above procedure was used to determine the moisture content in each case.

3.4.2 Increasing the Moisture Content of the Silt Lens

Using the relationship developed in Equation 3.1, the amount of water needed to attain desired moisture content was calculated. Two different moisture contents were used in addition to the residual moisture content of 2%. These were 14% and 7% to cover the range of moisture content observed at the site (Hartman *et al.*, 2004). Equation 3.2 was used to calculate the quantity of de-ionized water to be added to the silt.

$$W_w = (M.C. / 100) \times W_s \quad (3.2)$$

The calculations were made for 100 grams of silt and then applied to the quantity of silt used in preparing the lens. The residual moisture content of the silt was measured before starting the above procedure. Glass mason jars (950 mL) were used to mix the silt and de-ionized water and age it before use. Silt from the bucket was weighed and added to the glass jars and then mixed thoroughly with the calculated amount of deionized water using a stainless steel rod. The glass jars were then sealed and placed on a rotary mixer (equipped with a Daytona 3 speed motor) at 5 rpm for 24 hours. Experiments conducted earlier showed that a 24-hour slow mixing period was found adequate to attain uniform moisture content in the silt mass. The moisture content of the silt was determined after adding the de-ionized water and before sealing the glass jars.

3.5 SAMPLE ANALYSIS

The carbon tetrachloride samples were analyzed using a gas chromatograph (GC). Two such GCs were used, a SERIES II (Hewlett Packard, model 5890), equipped with a Thermal Conductivity Detector (TCD) and an Electron Capture Detector (ECD) and a SERIES II PLUS (Hewlett Packard, model 5890E) equipped with a Flame Ionization

Detector (FID) and an Electron Capture Detection (ECD). The principle of operation for each detector has been provided in Appendix C.

The different detectors were used depending on the concentration of the samples being analyzed. For concentrations ranging from saturation concentration (~ 129,000 ppm) to a low of 11 ppm, the TCD was used. For concentrations between 11 ppm and 5 ppm, the FID was used. For concentrations below the detection limit of the FID and down to 50 ppb, the ECD was used. A three point standard curve was generated for each day of sampling. For each standard concentration, triplicate injections were made. Two types of capillary GC columns used for the separation and analysis of carbon tetrachloride bases on the different phases in which analysis was carried out.

Flow cell experiments were conducted for a period of ~24 days on an average, following which the pump was shut down. Mass recovery calculations were conducted to measure the quantity of carbon tetrachloride recovered from the system. The data from these experiments is presented in Appendix A. Based on these mass recovery calculations, 92%- 97% of the carbon tetrachloride was removed from the silt lens. In order to close the mass balance it was necessary to extract the remaining carbon tetrachloride from the silt particles. A review of the existing methods used for liquid extractions was conducted and the process of accelerated solvent extraction was selected based on the speed and efficiency of extraction (Kenny et al., 1998; Heemken et al., 1997). An accelerated solvent extractor (ASE) (Dionex Inc, model ASE-200) was used for all extractions. The principle of working and the theory of the extractor are described in the Appendix D.

At the end of the experiment (24 days on an average), the lid of the cell was opened and the silt lens was then excavated carefully from the sand media. Sand was

removed using a vacuum until the upper surface of the silt lens was in sight. The sand around the sides of the lens was scooped out to expose the silt lens. Care was exercised during the extraction to ensure that the geometry of the lens was not disturbed. Samples were taken from nine locations along the cross section of the silt lens and these were tested for their moisture content using the procedure described in Section 3.4.1. The remaining silt lens was then packed into clean one-quart glass mason jars, sealed and then frozen (at -4°C) for extraction later.

Silt samples (10 g) were packed into stainless steel ASE cells sandwiched between sand layers (15 g each) and then extracted using Decane as the solvent (Acros Organics, 99 +%) at a temperature of 150°C and pressure of 1500 psi. After extraction, the solvent in the VOA vial was vortexed (Thermolyne Inc., MaxiMax Plus) to obtain a well-mixed sample and the volume was measured. A representative sample of the solvent (containing trace carbon tetrachloride) was then placed in 2mL crimp vials and analyzed through a GC using the automated sampler (Hewlett Packard, model 7673) for liquid injections.

3.5.1 Analysis with the TCD

The TCD was adjusted at the 'low sensitivity' for all concentrations above 50,000 ppm and saturation concentration. The detector was later switched to 'high sensitivity' for all concentrations between 50,000 ppm and 11 ppm. The carrier gas was nitrogen (99.9 % purity) while the auxiliary gas was helium (90.9% purity). Table 3.3 lists the pertinent parameters for the method used for analysis of carbon tetrachloride on the TCD.

Table 3.3 - Parameters for analysis method on the TCD (High and Low sensitivity).

Parameter	Value
Oven temperature	150 °C
Detector temperature	250 °C
Run time	5 minutes
Carbon tetrachloride peak eluted at	~ 3.0 minutes
Carrier gas flow	5.0 mL/min
Auxiliary flow	2.5 mL/min

3.5.2 Analysis with the FID

The carrier gas and the make up gas were nitrogen (99.9 % purity). For the flame a combination of air (99 % purity) and hydrogen (99 % purity) were used. Table 3.4 lists the pertinent parameters for the method used for analysis of carbon tetrachloride on the FID.

Table 3.4 - Parameters for analysis method on the FID.

Parameter	Value
Oven temperature	150 °C
Detector temperature	250 °C
Injection temperature	120 °C
Run time	5 minutes
Carbon tetrachloride peak eluted at	~2 minutes
Carrier gas flow	2.5 mL/min

3.5.3 Analysis with the ECD

The carrier gas and the make up gas were nitrogen (99.9 % purity). Table 3.5 lists the pertinent parameters for the method used for analysis of carbon tetrachloride on the ECD.

Table 3.5 - Parameters for analysis method on the ECD.

Parameter	Value
Oven temperature	150 °C
Detector temperature	250 °C
Injection temperature	120 °C
Run time	5 minutes
Carbon tetrachloride peak eluted at	~2 minutes
Carrier gas flow	2.5 mL/min
Bypass gas flow	1.5 mL/min

3.6 TRACER GAS TESTS

Inert tracer (Sulfur hexafluoride (SF₆)) tests were performed each time the cell was packed with a fresh silt lens and at the end of each run to ensure that the system characteristics were comparable between and after runs. During the tracer experiments a coil (~ 8 mL) of 5 mm (1/8 in) flexible stainless steel tubing was attached to the inlet through a 5 mm (1/8 in) stainless steel ‘T’ connection to provide sufficient sweep volume. A 5 mm (1/8 in) plug nut with a septum was used to inject the tracer vapor. The sweep volume ensured that there was no back flow of injected tracer gas. An 8 mL pulse of 31 ppm SF₆ standard (Scott Specialty Inc.) was injected into the inlet port of the cell. Cell effluent sampling commenced immediately with quantification by GC/ECD. Initially samples were taken at 6-minute intervals but the frequency was decreased after the peak concentration on the desorption curve for SF₆ was achieved. The frequency was decreased gradually to 10 minutes during the immediate downward slope after the peak and then to 20 minutes during the flattening of the curve. Sampling was continued for at least 3 residence times.

A 3-point standard curve was generated before and after the sampling using standards made from a calibrated standard from Scott Specialty. The preparation of standards has been discussed in Appendix B. The range of the standard curve was between 914 and 6,000 parts per trillion (ppt). A calibration curve was plotted from which the concentrations of the effluent SF₆ vapors were calculated and plotted versus time. The resulting concentration vs. time curve was used to calculate the actual residence time of the tracer within the system. By comparing the measured value to the theoretical value of the residence time, one could determine the amount of dispersion within the cell and effective volume being used.

3.7 HEALTH AND SAFETY PRECAUTIONS

Carbon tetrachloride is highly toxic and irritating compound by means of inhalation, ingestion, and skin absorption. The lethal dose for ingestion is 5-10 mL, and the acute (10-hour) exposure limit by inhalation is 2 ppm. Severe acute or chronic exposures to carbon tetrachloride may pose serious health risks. Excessive exposure to carbon tetrachloride liquid or vapor may result in depression, gastrointestinal symptoms, and cardiac arrhythmias. The eyes and skin may also be affected with symptoms such as hazy and narrowed vision and itchy skin and rashes. Kidney and liver damage may also occur for severe acute or chronic exposure, and carbon tetrachloride is suspected as a human carcinogen.

All experiments were performed under a fume hood (Canopy type) with a velocity of 26 m/min. All handling of carbon tetrachloride liquid or vapor was also conducted under the fume hood. The entire experimental set up was placed under the hood to ensure safety in case of a vapor leakage. Gloves, lab coats, safety glasses, and a gas mask (3M

Corp., 7002S Dual Cartridge half face piece) were used at all times when handling carbon tetrachloride. Cartridges (3M Corp., 6001 NIOSH) for the gas mask were changed as per direction from the manufacturer.

Periodic laboratory ambient air samples were analyzed for residual carbon tetrachloride vapors on the GC/ECD, which had the capability to measure concentration down to 50 ppb. These samples were collected in plastic syringes and injected into the GC. Personnel from the department of Environmental Health and Services, Washington State University, also conducted periodic checks for the ambient carbon tetrachloride vapors. The measured levels were well below the allowable standards of 2 ppm in the vapor phase.

4.0 RESULTS AND DISCUSSIONS

4.1 VAPOR EXTRACTION CELL

To understand the flow characteristics of the vapor extraction cell, tracer tests were performed using SF₆ gas. An 8 mL pulse of SF₆ was injected into the cell as described earlier in Section 3.3. Effluent samples were measured for a period of at least three times the residence time in the cell. The flow rate through the cell was set at ~ 309 mL/min, which corresponds to the flow rate used for all carbon tetrachloride vapor extraction experiments. Based on the flow rate and assumed porosity of 40 %, an estimated pore volume of ~ 51 liters, the theoretical residence time was calculated to be 162 min. The actual residence time was also calculated using SF₆ concentration-time data and the following equation:

$$\bar{t} = \frac{\sum(\Delta t_i) \cdot t_i \cdot C_i}{\sum(\Delta t_i) \cdot C_i} \quad (4.1)$$

Where

\bar{t} = mean residence time, min;

t_i = time, min;

C_i = SF₆ concentration, ppt; and

Δt_i = time interval between successive sample events, min.

The average residence time calculated from Equation 4.1 for all SF₆ runs was 150 min. Mass balance calculations were performed at the end of each experiment for the extraction efficiency of the system. A total mass of 42 mg was injected for each tracer test. An average of 29.4 mg was recovered from the system. This corresponds to 70 % recovery

of the injected tracer. Figure 4.1 shows a typical tracer test concentration-time profile.

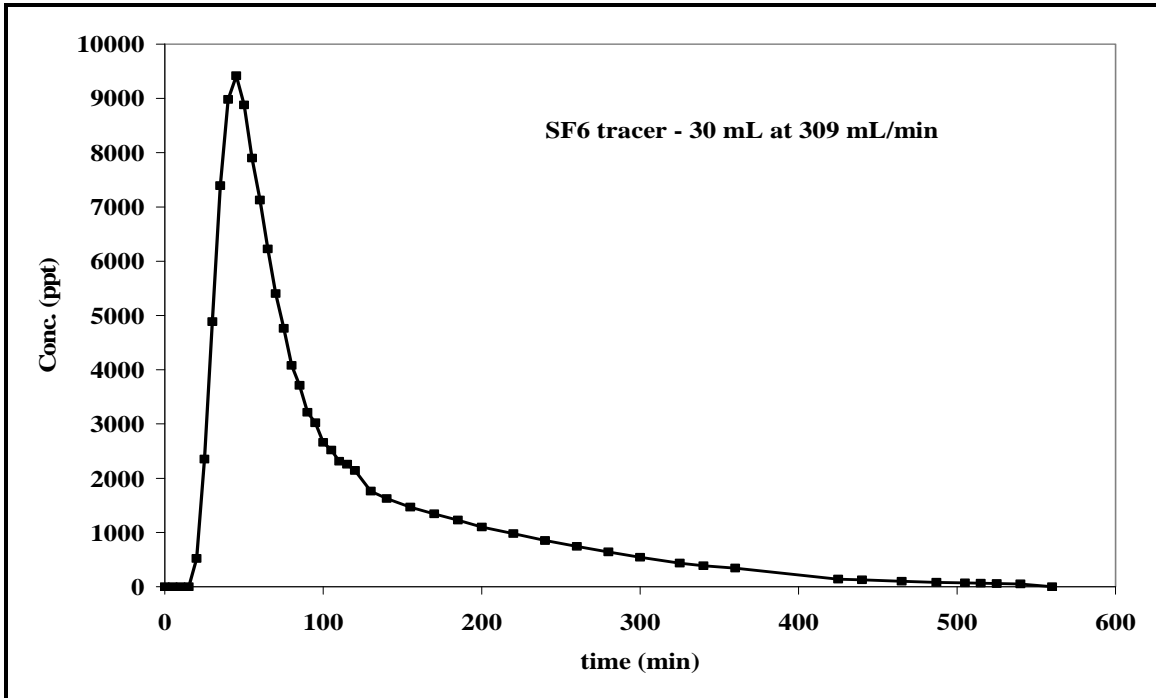


Figure 4.1 - Typical concentration vs. time curve from a tracer test.

4.2 EFFLUENT CONCENTRATION DATA

For the carbon tetrachloride extraction experiments, the effluent concentrations in the exit stream were monitored regularly. Samples from the exit stream were analyzed in a GC and the carbon tetrachloride that separated out from the injected sample was recorded as a response peak on a chromatogram. The chromatogram was integrated to obtain the area under the curve. These area counts were then used to calculate the concentration in the exit stream using information obtained from standard curves. The standard curves were developed independently on each day of sampling by analyzing factory certified standards of known concentrations. Figure 4.2 describes a sample chromatogram indicating the ‘response peaks’ for air and carbon tetrachloride.

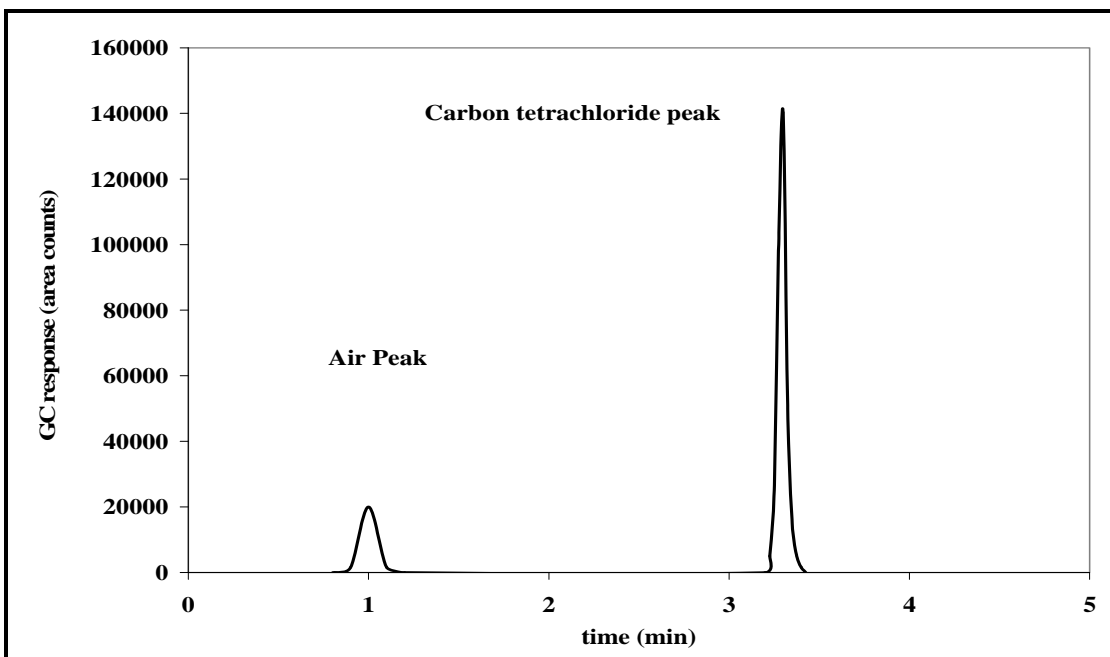


Figure 4.2 - Typical chromatogram obtained as GC response (analysis time = 5 min).

The concentrations calculated are plotted against time for the duration of the experiment. The resulting plot is a 'concentration-time profile' which shows the rate at which carbon tetrachloride is leaving the system through the exit stream. The data was plotted on a log (Y axis) versus normal (X axis) graph so that the low ppm concentrations on the concentration-time profile can be observed after approximately the sixth day. If plotted on a normal scale, the profile after approximately the sixth day gives the impression of merging with the X axis. Figure 4.3 shows a typical 'concentration-time profile'.

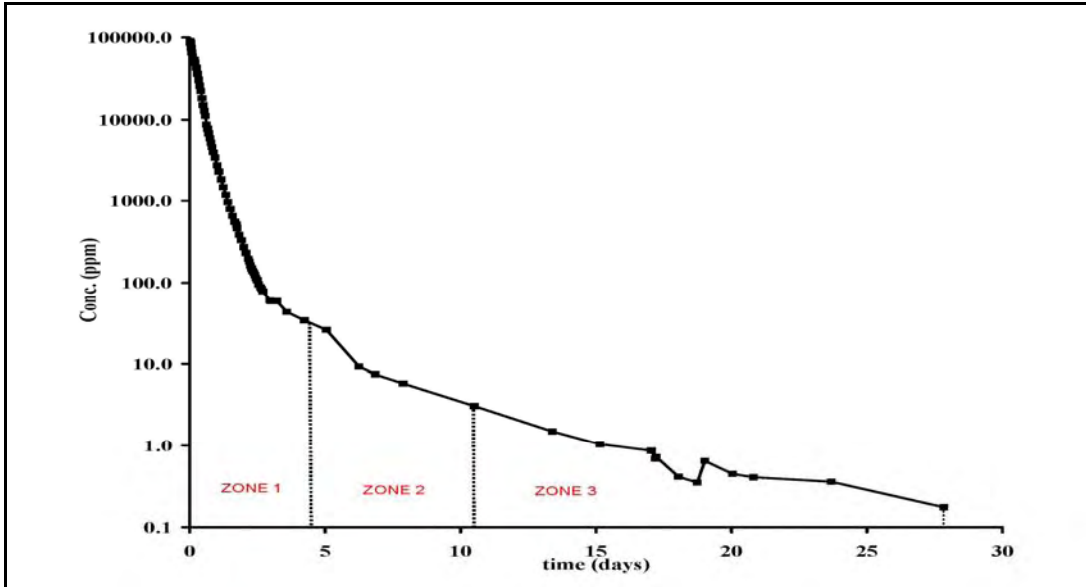


Figure 4.3 - Typical concentration-time profile for desorption of carbon tetrachloride showing various zones.

The concentration-time profile in Figure 4.3 can be described as ‘asymptotic’ in nature, recording high initial concentrations followed by low concentrations, which may continue for long periods (up to several months). In order to understand the desorption process represented by this profile; it was helpful to divide the profile into three sections or zones.

The profile in Figure 4.3 can be interpreted as the rate at which the mass of carbon tetrachloride is being removed from the system. This rate can be calculated as the product of the mass recovered at each sampling event and the flow rate through the system at that time. The removal rate was higher at the start of the extraction process (>85 mg/min) but gradually slows down as seen in Figure 4.3.

The first zone is characterized by near saturation concentrations of carbon tetrachloride and high values of rate of mass removed. It typically lasts for the first 4 days from the start of sampling during which the removal rate was observed to be in the range

of 270 mg/min to 1mg/min. This initial segment of this zone, which lasts for the first 5 hours, represents the sweeping away of all vapors that had accumulated over the 24 hour “resting” period that followed the injection of carbon tetrachloride. In the next segment of this zone, which typically lasts over the next 8 hours, the removal rate begins to drop (between 120 mg/min and 25 mg/min). As the vapors formed during the ‘resting’ period are swept away, further volatilization of the remaining carbon tetrachloride and subsequent removal of these vapors takes place within the cell.

The subsequent zones, Zone 2 and 3, account for a small percentage (<5%) of the total carbon tetrachloride removed from the system. For these zones the rate of mass removed is less than 1 mg/min. Data for concentration of carbon tetrachloride in the effluent stream for all experiments is presented in Appendix A. From the measured effluent concentrations, the mass of carbon tetrachloride extracted from the system was also calculated for each sampling event using the following equation (Nelson *et al*,1992):

$$M = \frac{P}{RT} * \frac{C_{\text{ppm}}}{10^6} * MW * Q * t \quad (4.2)$$

Where

M = Mass, mg;

P = atmospheric pressure, atm;

R = Ideal Gas Law Constant, 0.082061-atm/mole- °K ;

T = temperature, °K ;

C_{ppm} = effluent concentration, ppm;

MW = molecular weight of the contaminant gas, g/mole;

Q = flow rate, L/min; and

t = time, hours.

4.3 DATA DISCUSSION FOR EXTRACTION EXPERIMENTS

Experiments were conducted at three different moisture contents (2 %, 7 %, and 14 %) of the silt lens. This section presents a summary of the data from each experiment.

4.3.1 Experiments with silt lens moisture content at 2.03% and 2.04%

Duplicate experiments were conducted, the first with the moisture content of silt lens at 2.03 % and the second with silt moisture content at 2.04 %. The first experiment lasted 10.13 days while the second lasted for 15.25 days. The flow rate for the first experiment was 315 mL/min while that for the second was 305 mL/min. The ‘resting’ period for the first experiment was 28.5 hours while that for the second experiment was 24 hours. The concentration-time profiles from the two replicate runs are shown in Figure 4.4.

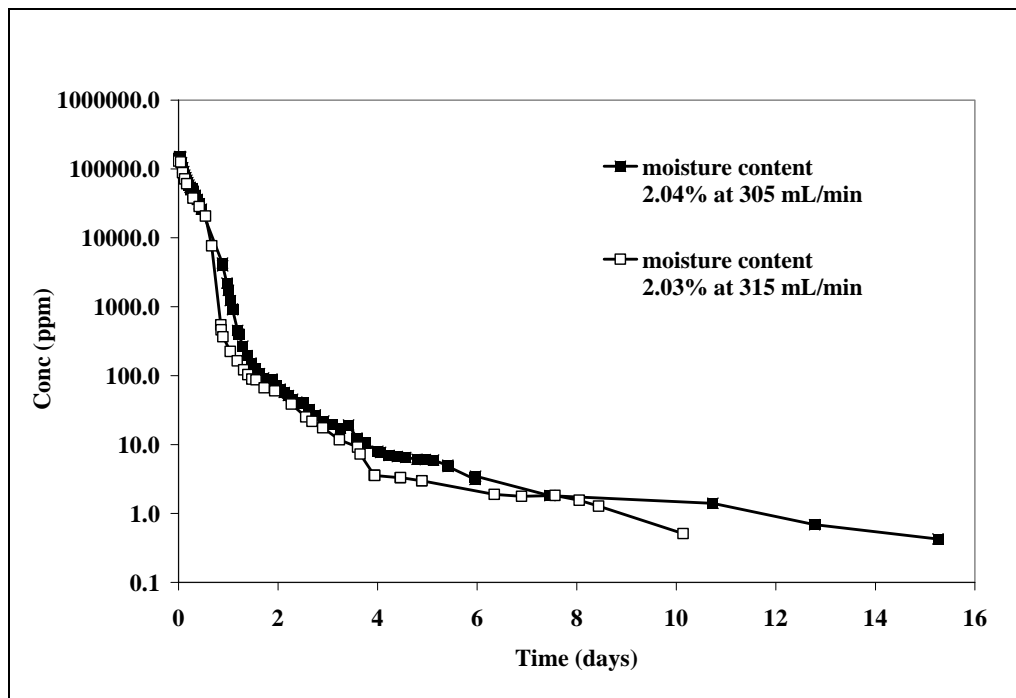


Figure 4.4 – Concentration-time profiles for replicate runs. First run at 2.04 % moisture content and 305 mL/min. Second run at 2.03% moisture content and 315 mL/min.

Zone 1 (approximately first 4 days) on the concentration-time profile exhibits fairly good similarity for the rate of desorption between the two experiments indicating good repetition between the two experiments. In Zone 2, the experiment with the 2.04% moisture content silt lens shows a slightly faster rate as compared to the one with 2.03% moisture content silt lens.

No comparisons could be made for Zone 3 as no data points were collected for the 2.03% experiment after day 11. The lowest measured concentration for the 2.03% moisture content experiment was 0.5 ppm on the 10th day while for the 2.04% moisture content experiment it was 0.4 ppm measured on the 15th day.

4.3.2 Experiments with silt lens moisture content at 7.35% and 7.73%

Duplicate experiments were conducted, the first with the moisture content of silt lens at 7.35 % and the second with silt moisture content at 7.73 %. The first experiment lasted 13.5 days while the second lasted for 27.84 days. The flow rate for the both experiments was 309 mL/min and the 'resting' period for both experiments was 24 hours. The concentration-time profiles for both experiments are shown in Figure 4.5.

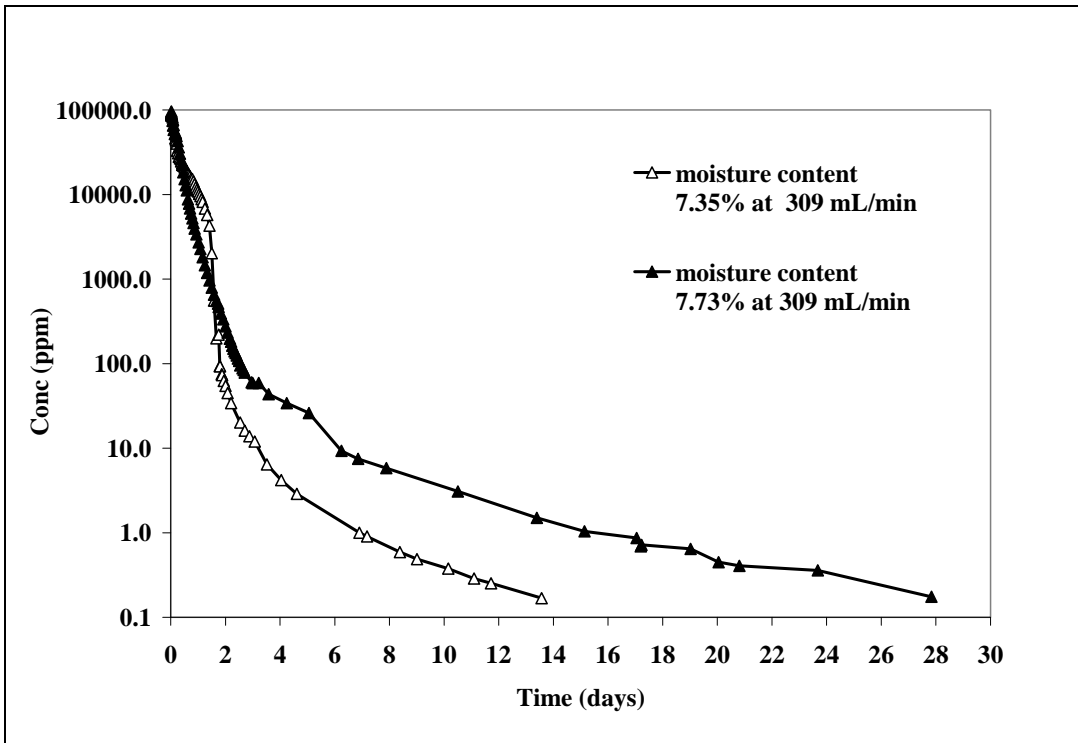


Figure 4.5 – Concentration-time profiles for replicate runs. First run at 7.35 % moisture content and second run at 7.73% moisture content. Both experiments were conducted at flow rate of 309 mL/min.

The initial segment (first day) of Zone 1 shows overlapping indicating fairly good repetition between the two experiments. However for the remainder of Zone 1, the two removal rates do not exhibit much similarity. The rate of removal for the 7.35% experiment is observed to be faster but decreases subsequently compared to the 7.73% experiment. For Zone 2 the rate of removal for the 7.73% moisture content experiment was observed to be faster than the 7.35% moisture content experiment. No comparisons could be made for Zone 3 as no data points were collected for the 7.35% experiment after day 13.

4.3.3 Experiment with silt moisture content at 14.5%

A single experiment was performed at this value of moisture content. The concentrations from the effluent gas stream were measured for 24 days. The flow rate of

air stream through the cell was maintained at 309 mL/min. Figure 4.6 is a plot of the concentration-time profile for this experiment.

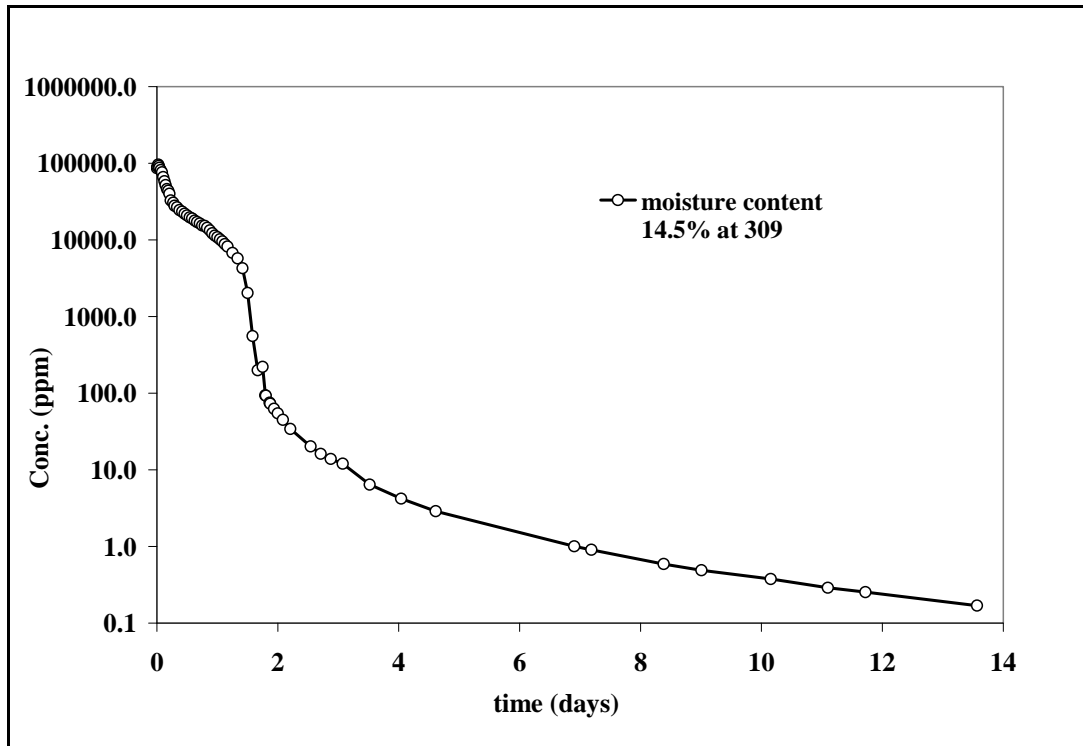


Figure 4.6 – Concentration-time profile for single run at 14.5 % moisture content and 309 mL/min.

The resting period for this experiment was 30 hours. The peak concentration for this experiment measured 30 min from start of sampling was 130,000 ppm. Zone 1 comprised of the first 4 days after the start of sampling with concentrations 68,000 ppm or higher. Zone 2 comprised of days 4 to 11 during which the concentrations ranged 68,000 ppm to 15,000 ppm. Zone 3 comprised of day 8 to day 24 when the pump was shut down. The concentrations ranged from 15,000 to 0.08 ppm.

4.4 MASS RECOVERY OF CARBON TETRACHLORIDE

The total mass of carbon tetrachloride recovered from the system during the vapor extraction was calculated for each run using the concentration-time profile. After the pump was shut down, the silt lens was extracted from the sand. A 10 g representative

sample was then used to recover trace carbon tetrachloride using the ASE method (decane as solvent) at 1,500 psi, 150 deg C for 450 minutes (5 cycles, 90 minutes each). This procedure has been described in detail in Chapter 3.0. The extracted liquid mixture was then analyzed in the GC to measure the trace carbon tetrachloride. However the process could not provide satisfactory results (recovery less than 5%) and hence the results were not used in calculations for mass recovery of carbon tetrachloride. Table 4.1 presents a summary of mass recovered from the different moisture content experiments.

Table 4.1 - Mass of carbon tetrachloride recovered.

Moisture content of silt lens (%)	Mass Recovered			
	Mass injected (mg/Kg)	Mass extracted (mg/Kg)	Mass remaining (mg/Kg)	Percentage removed (%)
2.04	29,197	27,499	1698	94
2.03	33,814*	32,455	1359	96
7.35	29,197	28,485	712	98
7.73	29,197	28,674	523	98
14.50	30,364	29,507	858	97

* - Mass remaining (4561.30 mg) from previous experiment was added to the mass injected (55 mL=88,000 mg) for this experiment.

4.5 MOISTURE CONTENT OF SILT LENS

Representative samples from the extracted silt lens were checked for moisture content. The procedure used for measuring the moisture content is described in Chapter 3.0. The moisture content of the silt particles (before and after) and loss of moisture content from during the experiment is presented in Table 4.2.

Table 4.2 – Moisture content of silt lens

Flow rate (mL/min)	Moisture content (%)		Loss in moisture content (%)
	Before experiment	After experiment	
305	2.03	2.01	<1.0
315	2.04	2.03	<0.5
309	7.35	6.21	15.5
309	7.73	6.76	12.5
309	14.5	7.70	46.8

4.6 INFLUENCE OF SILT MOISTURE

The desorption profile for all experiments was observed to follow a similar pattern with high initial saturation concentrations which after the first two days of sampling reduced to low values (< 280 ppm, except for the 14% run where the concentration was > 2000 ppm). The profile then flattened out resulting in very low-level concentrations (< 6 ppm, except for 7.73 % run where the value was 26 ppm) around the 5th day of the experiment. These low level concentrations persisted for several days giving the profile an extended tail along the X-axis. When the experiment was shut down the concentrations measured were < 0.5 ppm. A summary of the various zones for concentration-time profiles from all five experiments is provided in Table 4.3.

Table 4.3: Summary of the concentrations in each zone for all experiments:

Moisture content (%) and flow (mL/min)	Range of carbon tetrachloride concentrations (ppm)		
	Zone 1	Zone 2	Zone 3
2.03 & 315	130,000 to 3.5	3.5 to 0.51	No data points
2.04 & 305	141,000 to 10.5	8.0 to 1.5	1.4 to 0.42
7.35 & 309	86,500 to 6.42	4.19 to 0.28	0.25 to 0.16
7.73 & 309	86,600 to 43.0	34.0 to 3.0	3.0 to 0.17
14.5 & 309	12,000 to 6.64	6.2 to 0.30	0.26 to 0.08

The influence of soil moisture on the concentration-time profiles was observed to be inconsistent for the entire duration of experiments for the different initial moisture contents. With the exception of the initial segment (0-300 mins) in Zone 1, the concentration-time profiles did not exhibit similarities between the duplicate runs either. For the sake of discussion and data interpretation, the concentrations measured during the duplicate experiments were averaged by fitting them to a model using MS Excel based, Solver. The model generated a good fit for the 2.03 % and 2.04 % moisture content data, but did not present a good fit for the 7.35 % and 7.73 % moisture content data.

Instead, the concentration-time profiles for all five experiments were normalized (using the concentration measured in the exit stream from the first sampling event during each experiment) and plotted against time. Concentration-time profiles for all five experiments are presented in Figure 4.7 with the normalized concentration ratio expressed on a logarithmic scale to properly represent the tailing phase of the concentration-time profiles.

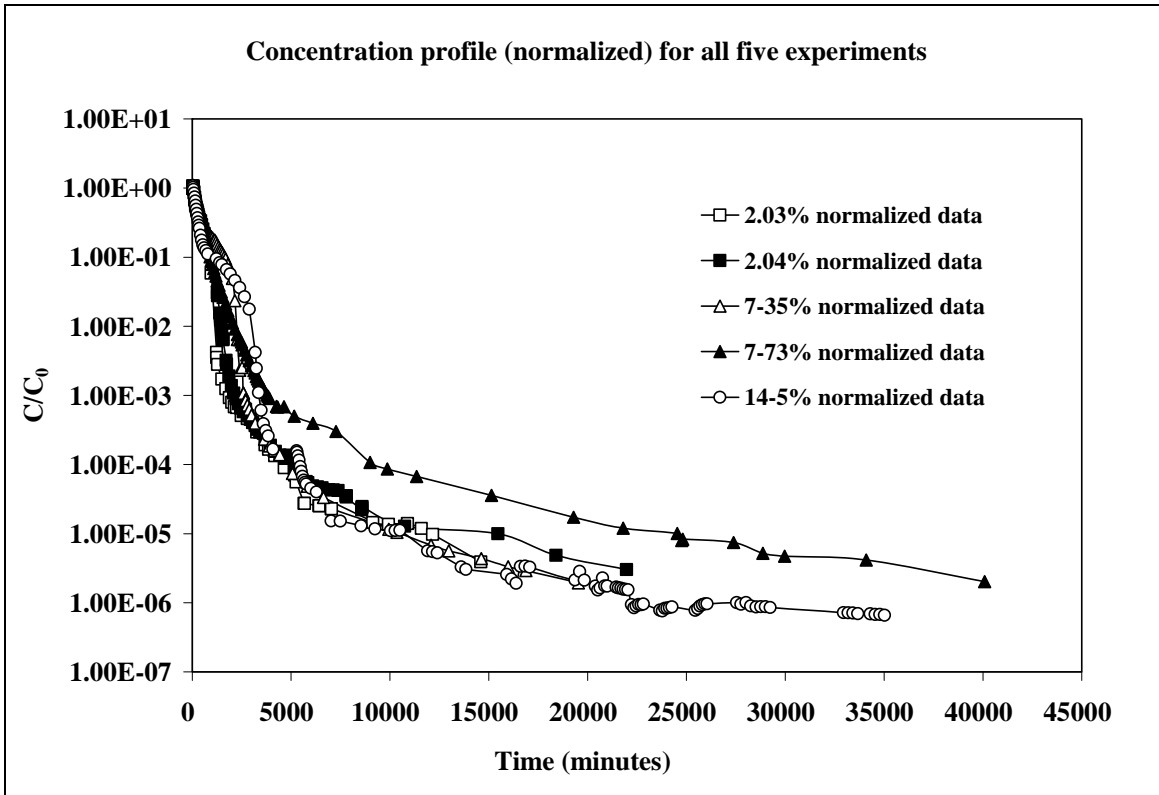


Figure 4.7 – Desorption profile for different moisture contents.

As explained earlier in Section 4.2, to discuss the similarities or differences between the concentration-time profiles from each experiment, the concentration-time profiles were divided in to smaller sections that exhibit similar trends. The following section discusses the characteristics of each zone as it relates to each concentration-time profile.

4.6.1 Zone 1

This zone includes the first 4 days from the first sampling event. During the initial stages of zone 1, near saturation concentrations formed during the ‘resting’ period were measured. Figure 4.8 represents the change in ratio of the measured concentration to the initial concentration with respect to time.

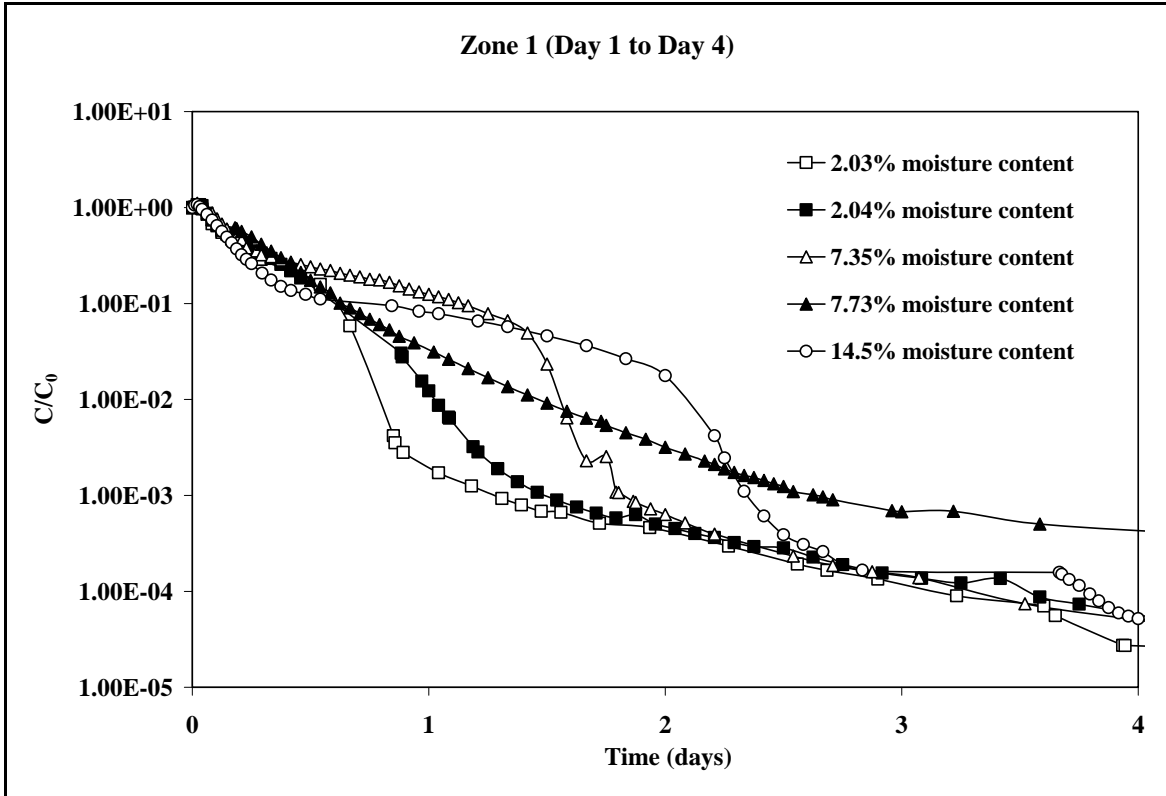


Figure 4.8 – Comparison of normalized concentrations in Zone 1.

The trend exhibited by the profile indicates that rate of loss is fairly similar for all experiments given the degree of variability in replicates.

4.6.2 Zone 2

This zone ranged between day 4 and day 11 from the first sampling event. Figure 4.9 represents the change in ratio of the measured concentration to the initial concentration with respect to time. The experiment with 2.03% moisture content is observed to exhibit a slightly slower loss in concentration compared to the other four experiments. However since the duplicate experiment performed at this moisture content does not exhibit similar behavior, the data does not provide any conclusive evidence on the effect of moisture content on removal of carbon tetrachloride from the system. The rate of loss of carbon tetrachloride from the system is nearly identical among all five experiments, again

providing no confirmation of interference of moisture content with the removal of carbon tetrachloride from the system for Zone 2.

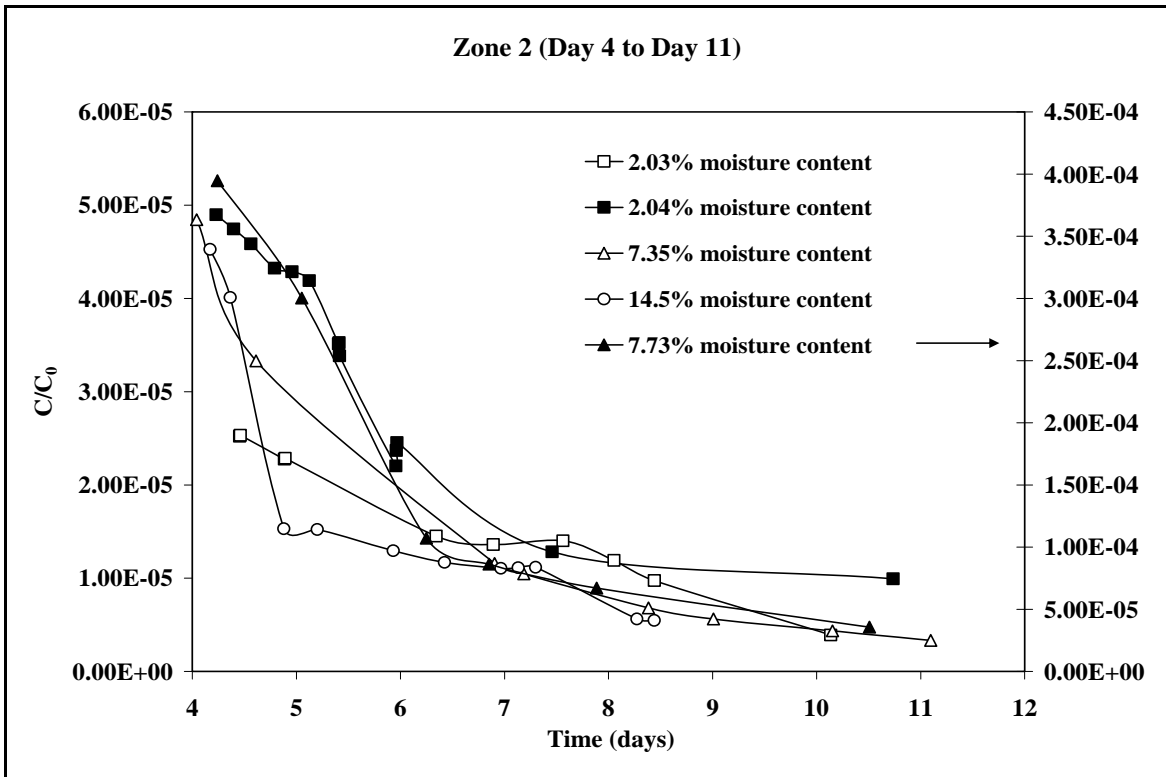


Figure 4.9 – Concentration-time profiles in Zone 2.

4.6.3 Zone 3

This zone ranges from day 11 after the first sampling event to the last sampling event. Figure 4.10 represents the change in ratio of the measured concentration to the initial concentration with respect to time. The experiment with the 14.5% moisture content is observed to exhibit a slower loss in concentration compared to the other four experiments. Although this would support the hypothesis that the increased moisture content contributes to the slower release of carbon tetrachloride vapors, since no duplicate experiment was performed at this moisture content it cannot be used as conclusive evidence to prove the hypothesis.

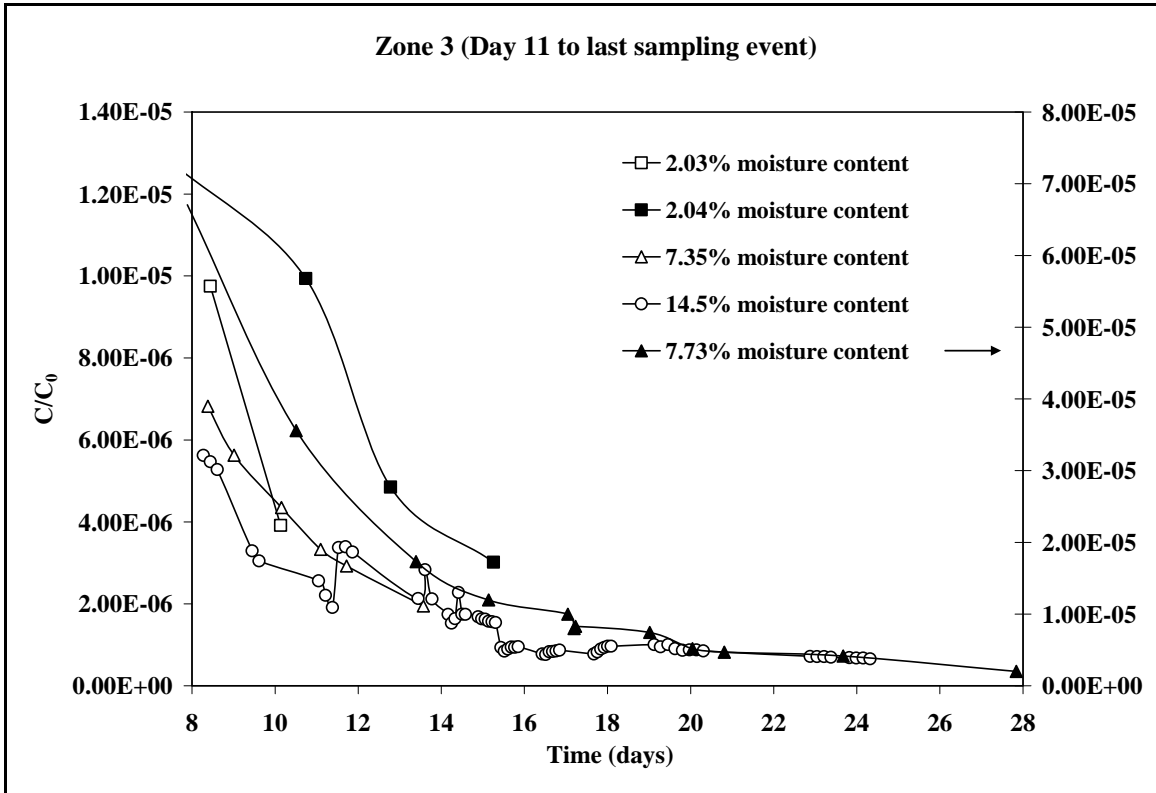


Figure 4.10 – Concentration-time profiles in Zone 3.

Samples taken from the silt lens used in the 14.5 % experiment, after the experiment was shutdown, showed an approximately 47% loss in total moisture content. Measurements taken during experiment did not indicate any significant changes in either relative humidity or temperature in the laboratory that housed the system. It is hence reasonable to assume that the air sweeping through the system was responsible for the loss in moisture content via partitioning of the water vapor into the air stream. The loss in moisture content for the other four experiments (2.04 %, 2.03 %, 7.73 %, and 7.35 %) was minimal and averaged at < 7 % total moisture during the experiment.

4.7 SUMMARY

The results from the tracer tests indicate that there was excellent distribution of air within the cell and no evidence of short-circuiting was found when the system was tested after sealing it. The average mass of carbon tetrachloride recovered from the system was approximately 97 %. The average mass of carbon tetrachloride remaining in the system from the five experiments was 1,030 mg/Kg.

For the vapor extraction experiments, carbon tetrachloride removal can be explained in three distinct phases. The first phase or Zone 1, where the vapors accumulated over the resting period are swept out of the system and the volatilization (which lasts for up to 5 hours after the first sampling event) of the free liquid carbon tetrachloride occurs within the silt lens . The second phase or Zone 2 on the concentration-time profile is representative of the inter-particle and intra-particle diffusion of the adsorbed carbon tetrachloride from the silt lens.

The final phase or Zone 3 represents the rate-limited removal of the persistent residual fraction of carbon tetrachloride. The presence of moisture in the silt lens probably caused a delay in the release of carbon tetrachloride from the silt particles to be available for partitioning in to the vapor phase. However the data does not provide much credibility to support this claim.

The resting period after injecting carbon tetrachloride in to the systems was at a minimum 24 hours and it allowed the system to attain elevated gas phase (near saturation) concentrations, with the carbon tetrachloride partitioning from the liquid to the vapor phase. The temperature in the laboratory around the system changed on a daily basis due to seasonal fluctuations in ambient temperature. Based on the average value of

ambient temperature measured during the five experiments (21.8 deg C), the saturation concentration of carbon tetrachloride should be in the vicinity of 129,000 ppm. The maximum value of the carbon tetrachloride concentrations for the duplicate experiments at 7.73 % and 7.35 % was measured to be 96,168 ppm. The experiments with 2.04 %, 2.03 %, and 14.5 % moisture content recorded values of maximum concentration in excess of the saturation concentration.

5.0 CONCLUSIONS AND RECOMMENDATIONS

The desorption profile for carbon tetrachloride at all soil moisture contents is observed to be asymptotic in nature, showing faster rates of removal at the earlier stages, which then change to relatively slower rates of removal giving it a prolonged tailing feature. The maximum rate of removal occurred within 45 minutes of the first sampling event. The total mass recovered from the system over the five experiments averaged at 97%, with almost 85% being recovered within the first few days, while the remainder was recovered over a longer period (several days) at a relatively slow rate.

The slower removal rates are indicative of the slow intra and inter-particle diffusion from the silt particles. The tailing suggests that the overall time required in removing the entire resistant fraction from the silt lens could be in the order of several months. This cleanup time when translated to field-scale systems could equal several years.

The presence of moisture in the system is observed to have an effect on the desorption process. The data suggests that there is a likely impact on the concentration-time profiles for Zones 3, further delaying the rate-limited removal of the resistant carbon tetrachloride fraction. The effect of moisture is however not consistent over the duration of the experiment. In the early stages of desorption, there is no evidence to suggest the effect of moisture content on rate of removal of carbon tetrachloride from the system.

However when the removal of the pure phase is accomplished, the water molecules within the silt lens provide resistance to the diffusion of the adsorbed component of carbon tetrachloride into the vapor phase. The efficiency of cleanup drops significantly as the carbon tetrachloride molecules have to overcome additional resistance to partition in to

the vapor phase to be available for removal.

SVE is thus observed to have limited use for the cleanup of the resistant carbon tetrachloride fraction in the vadose zone. Although the process removes almost 97 % of the carbon tetrachloride, the average soil concentration was 1030 mg/Kg. Continuous extractions to remove the remaining carbon tetrachloride result in low removal efficiency coupled with high energy and operation costs. As an alternative, the passive soil vapor extraction technique is recommended.

Passive soil vapor extraction uses the principle of pressure differences between the atmosphere and the subsurface to facilitate movement of carbon tetrachloride vapors to the surface where they can be treated. This system uses the underground pipe network created for the SVE process and a surface unit for treating the vapors before releasing them into the atmosphere, considerably reducing energy and operation costs.

RECOMMENDATIONS FOR FUTURE WORK

The use of passive soil vapor extraction for the removal of the resistant fraction should be investigated. The duration of shutdown has an impact on the equilibrium concentrations within the system and results in an increase in removal efficiency. The impact of PSVE under moist conditions could also be investigated.

The effect of age of the contaminant in the environment has an effect on the cleanup effort. The effect of contaminant age under conditions of moisture content above the ambient levels could be investigated in order to better our understanding of the desorption of the resistant fraction of carbon tetrachloride in the vadose zone.

BIBLIOGRAPHY

- Armstrong, J.E.; Frind, E.O.; and McClellan, R.D. (1994) Nonequilibrium Mass Transfer Between the Vapor, Aqueous, and Solid Phases in Unsaturated Soils During Vapor Extraction. *Water Res.*, **30**, 355.
- Bailey, S. J.; Baldini, N. C.; Barkley, E. I.; King, S. T.; Peters, K. A.; Rosiak, J. L. (2003) Annual Book of ASTM Standards: *Standard Test Methods for Laboratory Compaction of Soil Using Standard Effort (D698 – 00a)*. ASTM, v **04.08**, pg 78.
- Baklanov, M. R.; Mogilnikov, K. P.; Polovinkin, V.G.; and Dultsev, F. N. (2000) Determination of Pore Size Distribution in Thin Films by Ellipsometric Porosimetry. *J. Vac. Sci. Technol.*, **B 18**(3), 1385.
- Benson, W.B.; and Farquhar, G.J. (1992) Experiments on Movement of Vapor in Unsaturated Soil. *Subsurface Contamination by Immiscible Fluids: Proc. Int. Conf.*, Calgary, Canada. A.A Balkema, Rotterdam, Brookfield. Pg 115.
- Bloes, M. B.; Rathfelder, K. M.; and Mackay, D.M. (1992) Laboratory Studies of Vapor Extraction for Remediation of Contaminated Soil. *Subsurface Contamination by Immiscible Fluids: Proc. Int. Conf.*, Calgary, Canada. A.A Balkema, Rotterdam, Brookfield. Pg 255.
- Brusseau, M.L.; Popovicova, J.; and Silva, J.K. (1997) Characterizing Gas-Water Interfacial and Bulk-Water Partitioning for Gas-Phase Transport of Organic Contaminants in Unsaturated Porous Media. *Environ. Sci. Technol.*, **31**, 1645.
- Chen W.; Kan A. T.; and Tomson M. B. (2000) Irreversible Adsorption of Chlorinated Benzene to natural Sediments: Implications for Sediment Quality Criteria. *Environ. Sci. Technol.*, **34**, 385.
- Cho, H.J.; and Jaffe, P.R. (1990) The Volatilization of Organic Compounds in Unsaturated Porous Media During Infiltration. *J. Cont. Hydrol.*, **6**, 387.
- Falta, R.W.; Pruess, Karsten; and Chestnut, D.A. (1993) Modeling Advective Contaminant Transport During Soil Vapor Extraction. *Ground Water*, **31**, 1011.
- Farrell James and Reinhard Martin (1994) Desorption of Halogenated Organics from Model Solids, Sediments, and Soil Under Unsaturated Conditions. 1. Isotherms. *Environ. Sci. Technol.*, **28**, 53.
- Farrell James and Reinhard Martin (1994) Desorption of Halogenated Organics from Model Solids, Sediments, and Soil Under Unsaturated Conditions. 2. Kinetics. *Environ. Sci. Technol.*, **28**, 63.

- Ford, H.L. (1996) Impact of a Low Velocity Field on Soil Vapor Extraction of Carbon Tetrachloride. M.S. thesis, Washington State Univ., Pullman, Washington.
- Hartman, M. J.; Morasch, L. F.; and Webber W. D. (2004) PNNL-14548-SUM. (March 2003) Hanford Site Groundwater Monitoring for fiscal Year 2003. Pacific Northwest National Laboratory (PNNL), Richland, Washington.
- Heemken, O.P.; Theobald, Norbert; and Wenclawiak, B. W. (1997) Comparison of ASE and SFE Soxhlet, Sonication, and Methanolic Saponification Extractions for the Determination of Organic Micropollutants in Marine Particulate Matter. *Anal. Chem.*, 69, 2171.
- Holtz, R.D., and Kovacs, W.D (c1981) *An Introduction to Geotechnical Engineering*. Prentice-Hall Inc., NJ.
- Hughes, B.M.; Gillham, R.W.; and Mendoza,C.A. (1992) Transport of Trichloroethylene Vapors in the Unsaturated Zone: A field Experiment. *Subsurface Contamination by Immiscible Fluids: Proc. Int. Conf., Calgary, Canada*. A.A Balkema, Rotterdam, Brookfield. Pg 81.
- Kan, A.T.; Fu, G.; and Tomson, M.B. (1994) Adsorption/ Desorption Hysteresis in Organic Pollutant and Soil/ Sediment Interaction. *Environ. Sci. Technol.*, 28, 859.
- Kenny, D.V.; and Olesik, S. V. (1998) Extraction of Bituminous Coal Fly Ash for Polynuclear Aromatic Hydrocarbons: Evaluation of Modified and Unmodified Supercritical Fluid Extraction, Enhanced Fluidity Solvents, and Accelerated Solvent Extraction. *J. Chromatogr. Sci.*, 36, 66.
- Konstantinou I. K.; and Albanis T. A. (2000) Adsorption- Desorption Studies of Selected Herbicides in Soil-Fly Ash Mixtures. *J. Agric. Food Chem.*, 48, 4780.
- McClellan, R. D. (1991) Vapor Extraction of Trichloroethylene Under Controlled Field Conditions. M.Sc. thesis, Univ. of Waterloo, Waterloo, Ontario, Canada.
- McClellan, R.D.; and Gillham, R.W. (1992) Vapor Extraction of Trichloroethylene Under Controlled Conditions at the Borden Site. *Subsurface Contamination by Immiscible Fluids: Proc. Int. Conf., Calgary, Canada*. A.A Balkema, Rotterdam, Brookfield. Pg 89.
- Mendoza, C.A.; and Frind, E.O. (1990) Advective-Dispersive transport of Dense Organic Vapors in the Unsaturated Zone. 1. Model Development. *Water Res.*, 26, 379.
- Nelson, G. O (c1992) *Gas Mixtures: Preparation and control*. Lewis Publishers, Inc., MI

- Nyer, E. K.; Kidd, D.F.; Palmer, P.L.; Crossman, T. L.; Fam, Sami; Johns II, F. J.; Boetlecher, Gary; and Suthersan, S. S. (1996) *In-situ Treatment Technology*. CRC Press LLC.
- O'Neil, M. J.; Smith, Ann; Heckelman, P.E.; Obenchain, J. R.; Gallipeau, J. R.; D'Arecca, M. A.; and Budavari, S. (2001) *The MERCK INDEX – An Encyclopedia of Chemicals, Drugs, and Biologicals*. Merck Research Laboratories, NJ. Pg 305.
- Patakioutas, Georgios; and Albanis, T. A. (2002) Adsorption- Desorption studies of alachlor, metolachlor, EPTC, chlorothalonil and pirimiphos-methyl in contrasting soils. *Pest. Manag. Sci.*, 58, 352.
- Pavlostathis, S. G.; and Jaglal, K. (1991) Desorptive Behavior of Trichloroethylene in Contaminated Soil. *Environ. Sci. Technol.*, 25, 274.
- Pavlostathis, S. G.; and Mathavan, G. N. (1992) Desorption Kinetics of selected volatile organic compounds from field contaminated soils. *Environ. Sci. Technol.*, 26, 532.
- Poston, T. M.; Hanf, R.W.; Dirkes, R. L.; and Morasch, L.F. (2003) PNNL-14295. Hanford Site Environmental report for the calendar year 2002. Pacific Northwest National Laboratory (PNNL), Richland, Washington.
- Stephens, Daniel; Kowall, Steve; van Genuchten, Rien; Looney, Brian; Borns, David; Ellis, Darwin; Wilson, John; and Ullo, John (2000) *The DOE Complex-Wide Vadose Zone Science & Technology Roadmap: Characterization, Monitoring and Simulation of Subsurface Contaminant Transport*. INEEL, Idaho.
- Tekrony, M.C. and Ahlert, R. C. (2001) Adsorption of chlorinated hydrocarbon vapors onto soil in the presence of water. *J. Haz. Mats.*, B84, 135.
- Thibaud Catherine; Erkey Can; and Akgerman Aydin (1993) Investigation of The Effect of Moisture on the Sorption and Desorption of Chlorobenzene and Toluene from Soil. *Environ. Sci. Technol.*, 27, 2373.
- Ward, A. L.; and Gee, G. W (2000) PNNL-13263. *Vadose Zone Transport Field Study: Detailed Test Plan for Simulated Leak Tests*. Pacific Northwest National Laboratory (PNNL), Richland, Washington.
- Ward, A. L.; Gee, G. W.; Zhang, Z.F.; and Keller, J.M. (2002) PNNL-14150. *Vadose Zone Transport Field Study: FY 2002 Status Report*. Pacific Northwest National Laboratory (PNNL), Richland, Washington.
- Wilkins, D.; Abriola, L. M.; and Pennell, K. D. (1995) Experimental Investigation of Rate –limited Nonaqueous Phase Volatilization in Unsaturated Porous Media: Steady State Mass Transfer. *Water Res.*, 31, 2159.

Wilson, J.L. (1992) Pore Scale Behavior of Spreading and Non-spreading Organic Liquids. Subsurface Contamination by Immiscible Fluids: Proc. Int. Conf., Calgary, Canada. A.A Balkema, Rotterdam, Brookfield. Pg 107.

Yonge, D. R.; Kelnath, T. M.; Pozanska, Kazimera; and Jiang, Z. P. (1985) Single-Solute Irreversible Adsorption on Granular Activated Carbon. Environ. Sci. Technol., 19, 690.

APPENDIX A

EXPERIMENTAL DATA

Table A.1
Data for 2.03 % moisture content experiment

Time			Conc	delt	Ci delt	ti Ci delt	ti2 Ci delt
mins	hrs	days	ppm				
0	0	0	141463.5	-	-	-	-
15	0.25	0.01	142814.0	15	13448703.8	201730556.8	3025958352.3
30	0.5	0.021	151432.8	15	14260338.3	427810149.8	12834304495.1
45	0.75	0.031	151731.0	15	14288417.1	642978768.1	28934044563.7
60	1	0.042	147994.3	15	13936537.2	836192233.1	50171533983.8
90	1.5	0.063	123521.7	30	23263922.7	2093753040.8	188437773674.4
120	2	0.083	104584.6	30	19697342.4	2363681085.1	283641730208.5
150	2.5	0.104	91260.6	30	17187915.3	2578187296.0	386728094396.0
180	3	0.125	81697.7	30	15386839.4	2769631097.6	498533597570.2
210	3.5	0.146	74507.5	30	14032652.0	2946856915	6.1884E+11
240	4	0.167	68652.8	30	12929987.5	3103196993	7.44767E+11
270	4.5	0.188	63354.6	30	11932120.0	3221672397	8.69852E+11
300	5	0.208	58582.2	30	11033297.6	3309989266	9.92997E+11
330	5.5	0.229	54221.8	30	10212076.4	3369985206	1.1121E+12
360	6	0.25	49885.4	30	9395345.8	3382324485	1.21764E+12
390	6.5	0.271	51640.0	30	9725815.3	3793067971	1.4793E+12
415	6.9	0.288	43206.9	25	6781274.3	2814228854	1.1679E+12
420	7	0.292	47501.6	5	1491064.7	626247179.7	2.63024E+11
480	8	0.333	41745.5	60	15724594.6	7547805403	3.62295E+12
540	9	0.375	36192.9	60	13633058.2	7361851433	3.9754E+12
600	10	0.417	31201.2	60	11752779.9	7051667957	4.231E+12
660	11	0.458	26102.1	60	9832082.3	6489174292	4.28286E+12
1272	21.2	0.883	4288.8	612	16478029.2	20960053172	2.66612E+13
1278	21.3	0.888	3921.4	6	147711.3	188775054.8	2.41255E+11
1398	23.3	0.971	2198.1	120	1655972.6	2315049696	3.23644E+12
1440	24	1	1738.6	42	458416.1	660119142.4	9.50572E+11
1500	25	1.042	1225.0	60	461417.9	692126919.5	1.03819E+12
1560	26	1.083	926.3	60	348917.0	544310489.6	8.49124E+11
1565	26.08	1.087	904.4	5	28388.7	44428382.94	69530419294

Table A.1
Data for 2.03 % moisture content experiment

Time			Conc	delt	Ci delt	ti Ci delt	ti2 Ci delt
mins	hrs	days	ppm				
1710	28.5	1.188	454.1	145	413331.4	706796688.7	1.20862E+12
1740	29	1.208	400.9	30	75501.3	131372270.4	2.28588E+11
1860	31	1.292	268.8	120	202497.0	376644475.7	7.00559E+11
1980	33	1.375	196.0	120	147687.7	292421713.7	5.78995E+11
2100	35	1.458	152.1	120	114580.7	240619502.7	5.05301E+11
2220	37	1.542	126.2	120	95098.0	211117667.9	4.68681E+11
2340	39	1.625	106.9	120	80506.8	188386007.9	4.40823E+11
2460	41	1.708	92.5	120	69679.1	171410571.5	4.2167E+11
2580	43	1.792	82.3	120	62006.6	159977090.9	4.12741E+11
2700	45	1.875	88.9	120	66991.7	180877456.2	4.88369E+11
2820	47	1.958	71.1	120	53575.2	151082133.8	4.26052E+11
2940	49	2.042	63.6	120	47945.6	140960146.6	4.14423E+11
3060	51	2.125	56.8	120	42799.5	130966345.7	4.00757E+11
3180	53	2.208	51.4	120	38687.7	123026957.8	3.91226E+11
3300	55	2.292	45.5	120	34248.5	113020057.6	3.72966E+11
3420	57	2.375	41.4	120	31166.0	106587717.4	3.6453E+11
3600	60	2.5	40.0	180	45244.1	162878883.7	5.86364E+11
3780	63	2.625	32.1	180	36324.1	137305130.5	5.19013E+11
3960	66	2.75	26.8	180	30289.1	119944662.6	4.74981E+11
4200	70	2.917	21.9	240	33045.6	138791604.9	5.82925E+11
4440	74	3.083	19.4	240	29157.4	129458873.1	5.74797E+11
4680	78	3.25	17.3	240	26048.9	121908899	5.70534E+11
4920	82	3.417	19.3	240	29053.4	142942929	7.03279E+11
5160	86	3.583	12.3	240	18605.2	96002620.14	4.95374E+11
5400	90	3.75	10.4	240	15694.2	84748652.07	4.57643E+11
5765	96.08	4.003	8.0	365	18334.4	105697761.6	6.09348E+11
5845	97.42	4.059	7.7	80	3859.1	22556361.31	1.31842E+11
6090	101.5	4.229	6.9	245	10655.3	64890655.42	3.95184E+11
6330	105.5	4.396	6.7	240	10115.5	64030986.88	4.05316E+11

Table A.1
Data for 2.03 % moisture content experiment

Time			Conc	delt	Ci delt	ti Ci delt	ti2 Ci delt
mins	hrs	days	ppm				
6570	109.5	4.563	6.5	240	9773.3	64210421.6	4.21862E+11
6900	115	4.792	6.1	330	12675.9	87463854.41	6.03501E+11
7140	119	4.958	6.1	240	9137.5	65241673.13	4.65826E+11
7380	123	5.125	5.9	240	8932.0	65917856.65	4.86474E+11
7785	129.8	5.406	5.0	405	12634.7	98361008.81	7.6574E+11
7791	129.9	5.41	5.0	6	187.9	1464045.868	11406381360
7797	130	5.415	4.8	6	180.3	1405752.888	10960655265
8577	143	5.956	3.1	780	15272.9	130995241.8	1.12355E+12
8584	143.1	5.961	3.4	7	147.3	1264671.158	10855937220
8591	143.2	5.966	3.5	7	152.6	1311290.129	11265293499
10741	179	7.459	1.8	2150	24465.9	262788596.3	2.82261E+12
15461	257.7	10.74	1.4	4720	41647.5	643911890.1	9.95552E+12
18401	306.7	12.78	0.7	2940	12660.9	232973237.7	4.28694E+12
21971	366.2	15.26	0.4	3570	9568.5	210228942.8	4.61894E+12
			SUM	21971	291565184.0	99020858745	9.90036E+13

Table A.2
Data for 2.04 % moisture content experiment

Time			Conc	delt	Ci delt	ti Ci delt	ti2 Ci delt
mins	hrs	days	ppm				
0	0	0	130481.48	-	-	-	-
60	1	0.042	126279.21	60	47566543.7	2853992621.4	1.7124E+11
120	2	0.083	88430.53	60	33309794.8	3997175379.8	4.79661E+11
180	3	0.125	71842.46	60	27061442.5	4871059654.1	8.76791E+11
240	4	0.167	61123.59	60	23023884.6	5525732300.2	1.32618E+12
420	7	0.292	37539.38	180	42420730.4	17816706748.2	7.48302E+12
600	10	0.417	28507.73	180	32214667.3	19328800362.9	1.15973E+13
780	13	0.542	20693.68	180	23384534.5	18239936941.8	1.42272E+13
960	16	0.667	7636.88	180	8629924.9	8284727898.4	7.95334E+12
1225	20.42	0.851	546.61	85	291687.4	357317070.5	4.37713E+11
1235	20.58	0.858	460.55	10	28913.4	35708016.0	44099399770
1285	21.42	0.892	365.73	50	114801.3	147519646.3	1.89563E+11
1500	25	1.042	224.09	215	302473.3	453710021.3	6.80565E+11
1700	28.33	1.181	163.26	200	204992.3	348486951.5	5.92428E+11
1885	31.42	1.309	121.12	185	140666.3	265155938.8	4.99819E+11
2005	33.42	1.392	103.65	120	78083.6	156557591.2	3.13898E+11
2125	35.42	1.476	89.28	120	67256.0	142919009.4	3.03703E+11
2245	37.42	1.559	86.78	120	65375.9	146768826.6	3.29496E+11
2480	41.33	1.722	66.62	235	98292.0	243764200.6	6.04535E+11
2785	46.42	1.934	60.19	305	115247.2	320963555.9	8.93884E+11
3265	54.42	2.267	38.54	480	116126.1	379151783.0	1.23793E+12
3685	61.42	2.559	25.15	420	66312.1	244360127.2	9.00467E+11
3865	64.42	2.684	21.63	180	24439.3	94457774.8	3.65079E+11
4175	69.58	2.899	17.53	310	34123.2	142464161.0	5.94788E+11
4655	77.58	3.233	11.71	480	35299.9	164320870.6	7.64914E+11
5185	86.42	3.601	9.17	530	30512.0	158204598.5	8.20291E+11
5255	87.58	3.649	7.30	70	3206.4	16849422.8	88543717054
5665	94.42	3.934	3.57	410	9190.5	52064053.3	2.94943E+11
5680	94.67	3.944	3.56	15	335.5	1905815.1	10825029504

Table A.2
Data for 2.04 % moisture content experiment

Time			Conc	delt	Ci delt	ti Ci delt	ti2 Ci delt
mins	hrs	days	ppm				
6415	106.9	4.455	3.29	735	15181.7	97390372.9	6.24759E+11
6425	107.1	4.462	3.30	10	207.4	1332560.9	8561704054
7035	117.3	4.885	2.97	610	11377.5	80040533.8	5.63085E+11
7045	117.4	4.892	2.98	10	187.3	1319798.3	9297979229
9135	152.3	6.344	1.89	1680	19980.3	182519959.0	1.66732E+12
9925	165.4	6.892	1.78	790	8808.8	87427563.8	8.67719E+11
10890	181.5	7.563	1.83	965	11074.9	120605148.0	1.31339E+12
11595	193.3	8.052	1.55	705	6872.5	79686283.3	9.23962E+11
12155	202.6	8.441	1.27	560	4472.7	54365286.4	6.6081E+11
14595	243.3	10.14	0.51	2440	7823.4	114182500.6	1.66649E+12
			SUM	14595	239202229.1	85241759717.1	6.19673E+13

Table A.3
Data for 7.35 % moisture content experiment

Time			Conc	delt	Ci delt	ti Ci delt	ti2 Ci delt
mins	hrs	days	ppm				
0	0	0	86643.30	-	-	-	-
15	0.25	0.01	90068.01	15	8159146.37	122387195.59	1835807934
30	0.5	0.021	90191.41	15	8481649.75	254449492.61	7633484778
45	0.75	0.031	88465.35	15	8493269.54	382197129.31	17198870819
60	1	0.042	85065.72	15	8330728.27	499843696.25	29990621775
90	1.5	0.063	74124.45	30	16021173.71	1441905634.10	1.29772E+11
120	2	0.083	65301.31	30	13960507.70	1675260923.56	2.01031E+11
150	2.5	0.104	58098.43	30	12298769.59	1844815439.00	2.76722E+11
180	3	0.125	52163.20	30	10942186.64	1969593594.83	3.54527E+11
210	3.5	0.146	44475.96	30	9824352.29	2063113981.29	4.33254E+11
240	4	0.167	37692.26	30	8376548.58	2010371659.33	4.82489E+11
260	4.3	0.181	53286.14	20	4732610.01	1230478603.03	3.19924E+11
270	4.5	0.188	52250.39	10	3345282.17	903226185.89	2.43871E+11
300	5	0.208	49000.34	30	9840774.47	2952232341.76	8.8567E+11
360	6	0.25	42782.29	60	18457328.52	6644638268.06	2.39207E+12
420	7	0.292	35979.37	60	16115127.17	6768353411.21	2.84271E+12
480	8	0.333	30409.51	60	13552620.07	6505257635.92	3.12252E+12
540	9	0.375	26035.60	60	11454579.75	6185473067.45	3.34016E+12
600	10	0.417	22408.80	60	9807024.54	5884214724.38	3.53053E+12
660	11	0.458	18294.46	60	8440891.91	5570988657.50	3.67685E+12
720	12	0.5	15150.28	60	6891111.03	4961599944.48	3.57235E+12
780	13	0.542	12855.33	60	5706768.71	4451279594.03	3.472E+12
840	14	0.583	11165.17	60	4842315.73	4067545212.08	3.41674E+12
900	15	0.625	8747.41	60	4205668.89	3785102003.09	3.40659E+12
960	16	0.667	7772.19	60	3294951.58	3163153519.55	3.03663E+12
1020	17	0.708	6822.67	60	2927608.93	2986161108.85	3.04588E+12
1080	18	0.75	5945.55	60	2569946.82	2775542560.59	2.99759E+12
1140	19	0.792	5230.63	60	2239556.68	2553094618.06	2.91053E+12
1200	20	0.833	4619.73	60	1970261.43	2364313711.25	2.83718E+12
1260	21	0.875	3953.38	60	1740147.11	2192585363.30	2.76266E+12
1350	22.5	0.938	3372.97	90	2233721.82	3015524450.80	4.07096E+12
1470	24.5	1.021	2711.22	120	2541046.12	3735337792.36	5.49095E+12
1560	26	1.083	2269.02	90	1531886.11	2389742327.53	3.728E+12
1680	28	1.167	1817.94	120	1709378.47	2871755832.38	4.82455E+12
1800	30	1.25	1463.22	120	1369556.86	2465202348.50	4.43736E+12
1920	32	1.333	1181.37	120	1102322.90	2116459961.03	4.0636E+12
2040	34	1.417	963.26	120	889993.38	1815586489.01	3.7038E+12

Table A.3
Data for 7.35 % moisture content experiment

Time			Conc	delt	Ci delt	ti Ci delt	ti2 Ci delt
mins	hrs	days	ppm				
2160	36	1.5	791.66	120	725673.29	1567454316.82	3.3857E+12
2280	38	1.583	652.94	120	596398.46	1359788496.41	3.10032E+12
2400	40	1.667	552.44	120	491891.91	1180540592.52	2.8333E+12
2490	41.5	1.729	512.32	90	312138.35	777224501.33	1.93529E+12
2520	42	1.75	466.45	30	96489.14	243152626.80	6.12745E+11
2640	44	1.833	390.71	120	351402.86	927703561.02	2.44914E+12
2760	46	1.917	334.18	120	294342.09	812384171.75	2.24218E+12
2880	48	2	274.79	120	251752.97	725048549.49	2.08814E+12
3000	50	2.083	233.34	120	207014.07	621042215.44	1.86313E+12
3120	52	2.167	197.69	120	175789.91	548464530.34	1.71121E+12
3180	53	2.208	182.21	60	74465.42	236800044.28	7.53024E+11
3240	54	2.25	163.23	60	68635.47	222378926.91	7.20508E+11
3300	55	2.292	150.48	60	61484.85	202900007.13	6.6957E+11
3360	56	2.333	140.02	60	56683.91	190457927.25	6.39939E+11
3420	57	2.375	133.04	60	52741.56	180376142.05	6.16886E+11
3480	58	2.417	124.33	60	50113.33	174394395.56	6.06892E+11
3540	59	2.458	114.62	60	46832.96	165788679.36	5.86892E+11
3600	60	2.5	107.61	60	43175.72	155432601.33	5.59557E+11
3660	61	2.542	95.22	60	40534.38	148355846.42	5.42982E+11
3780	63	2.625	88.00	120	71735.60	271160578.77	1.02499E+12
3840	64	2.667	83.86	60	33147.81	127287601.26	4.88784E+11
3900	65	2.708	78.35	60	31587.92	123192871.44	4.80452E+11
4260	71	2.958	60.19	360	177081.09	754365438.62	3.2136E+12
4320	72	3	58.67	60	22671.24	97939767.32	4.231E+11
4635	77.25	3.219	59.15	315	116021.30	537758725.57	2.49251E+12
5160	86	3.583	43.47	525	194941.32	1005897215.73	5.19043E+12
6108	101.8	4.242	34.20	948	258708.36	1580190691.92	9.6518E+12
7275	121.3	5.052	26.02	1167	250593.64	1823068757.12	1.32628E+13
9000	150	6.25	9.29	1725	281735.41	2535618683.42	2.28206E+13
9867	164.5	6.852	7.48	867	50564.29	498917890.77	4.92282E+12
11357	189.3	7.887	5.81	1490	69937.27	794263609.49	9.02029E+12
15131	252.2	10.51	3.08	3775	137671.21	2083158151.13	3.15211E+13
19287	321.5	13.39	1.50	4156	80447.08	1551582750.95	2.99254E+13
21800	363.3	15.14	1.04	2513	23666.04	515914912.77	1.12468E+13
24540	409	17.04	0.87	2740	17846.25	437946996.09	1.07472E+13
24762	412.7	17.2	0.69	222	1208.08	29914368.68	7.4074E+11
24811	413.5	17.23	0.72	48.6	210.71	5227791.81	1.29705E+11

Table A.3
Data for 7.35 % moisture content experiment

Time			Conc	delt	Ci delt	ti Ci delt	ti2 Ci delt
mins	hrs	days	ppm				
25984	433.1	18.04	0.41	1173	5300.28	137720248.32	3.57847E+12
26981	449.7	18.74	0.35	997.8	2589.58	69870405.41	1.8852E+12
27385	456.4	19.02	0.65	403.8	889.58	24361457.68	6.67143E+11
28865	481.1	20.05	0.45	1480	6001.61	173235335.53	5.0004E+12
29968	499.5	20.81	0.41	1103	3106.15	93083758.88	2.7895E+12
34091	568.2	23.67	0.36	4123	10560.06	359998439.48	1.22725E+13
40085	668.1	27.84	0.18	5995	13546.74	543026300.21	2.17674E+13
			SUM	40085	254260142.94	1.33233E+11	3.17247E+14

Table A.4
Data for 7.73 % moisture content experiment

Time			Conc	delt	Ci delt	ti Ci delt	ti2 Ci delt
mins	hrs	days	ppm				
0	0	0	86593.27	-	-	-	-
15	0.25	0.01	90676.52	15	8538952.67	128084290.10	1921264352
30	0.5	0.021	96168.36	15	9056115.20	271683455.9	8150503677
45	0.75	0.031	92539.06	15	8714346.79	392145605.7	17646552256
60	1	0.042	87500.39	15	8239857.95	494391476.8	29663488611
90	1.5	0.063	81589.20	30	15366410.44	1382976939	1.24468E+11
120	2	0.083	76011.25	30	14315864.85	1717903782	2.06148E+11
150	2.5	0.104	66189.86	30	12466116.32	1869917448	2.80488E+11
180	3	0.125	58389.57	30	10997020.02	1979463604	3.56303E+11
210	3.5	0.146	51902.88	30	9775324.94	2052818237	4.31092E+11
240	4	0.167	46096.33	30	8681726.69	2083614405	5.00067E+11
270	4.5	0.188	43728.58	30	8235786.46	2223662344	6.00389E+11
300	5	0.208	39933.34	30	7520996.47	2256298941	6.7689E+11
330	5.5	0.229	32812.90	30	6179941.97	2039380851	6.72996E+11
360	6.5	0.271	30635.84	30	5769916.78	2077170041	7.47781E+11
425	7	0.292	27923.41	65	11394633.06	4842719051	2.05816E+12
480	8	0.333	26696.19	55	9217867.31	4424576308	2.1238E+12
540	9	0.375	24539.93	60	9243639.91	4991565549	2.69545E+12
600	10	0.417	23337.27	60	8790627.14	5274376285	3.16463E+12
660	11	0.458	21975.89	60	8277826.16	5463365265	3.60582E+12
720	12	0.5	20898.11	60	7871849.95	5667731964	4.08077E+12
780	13	0.542	19747.88	60	7438582.55	5802094388	4.52563E+12
840	14	0.583	19077.31	60	7185994.41	6036235305	5.07044E+12
900	15	0.625	17867.96	60	6730457.61	6057411846	5.45167E+12
960	16	0.667	17116.49	60	6447396.93	6189501055	5.94192E+12
1020	17	0.708	16405.30	60	6179506.80	6303096932	6.42916E+12
1080	18	0.75	15460.27	60	5823538.15	6289421200	6.79257E+12
1140	19	0.792	15237.82	60	5739745.25	6543309583	7.45937E+12
1200	20	0.833	14366.16	60	5411409.59	6493691508	7.79243E+12
1260	21	0.875	13271.42	60	4999044.40	6298795947	7.93648E+12
1320	22	0.917	12226.93	60	4605609.52	6079404568	8.02481E+12
1380	23	0.958	11421.79	60	4302330.23	5937215715	8.19336E+12
1440	24	1	10813.62	60	4073247.22	5865475999	8.44629E+12
1500	25	1.042	10181.02	60	3834961.98	5752442973	8.62866E+12
1560	26	1.083	9555.68	60	3599411.12	5615081347	8.75953E+12
1620	27	1.125	8809.10	60	3318190.89	5375469246	8.70826E+12
1680	28	1.167	8188.44	60	3084401.60	5181794690	8.70542E+12

Table A.4
Data for 7.73 % moisture content experiment

Time			Conc	delt	Ci delt	ti Ci delt	ti2 Ci delt
mins	hrs	days	ppm				
1800	30	1.25	6787.34	120	5113280.83	9203905502	1.6567E+13
1920	32	1.333	5729.44	120	4316299.99	8287295987	1.59116E+13
2040	34	1.417	4268.48	120	3215680.28	6559987775	1.33824E+13
2160	36	1.5	2027.93	120	1527754.58	3299949885	7.12789E+12
2280	38	1.583	557.04	120	419645.46	956791650.2	2.18148E+12
2400	40	1.667	198.92	120	149856.04	359654498.1	8.63171E+11
2520	42	1.75	220.12	120	165831.54	417895477	1.0531E+12
2580	43	1.792	93.82	60	35341.47	91180992.3	2.35247E+11
2595	43.25	1.802	92.57	15	8717.64	22622267.76	58704784839
2685	44.75	1.865	75.19	90	42482.11	114064461.5	3.06263E+11
2700	45	1.875	73.04	15	6877.72	18569837.89	50138562298
2790	46.5	1.938	62.61	90	35375.56	98697810.17	2.75367E+11
2880	48	2	54.59	90	30842.21	88825556.75	2.55818E+11
3000	50	2.083	44.83	120	33771.70	101315111.6	3.03945E+11
3180	53	2.208	34.20	180	38645.08	122891362.9	3.90795E+11
3660	61	2.542	20.16	480	60755.98	222366885.3	8.13863E+11
3900	65	2.708	16.14	240	24317.70	94839030.04	3.69872E+11
4140	69	2.875	13.84	240	20847.75	86309670.14	3.57322E+11
4425	73.75	3.073	12.01	285	21485.29	95072417.09	4.20695E+11
5070	84.5	3.521	6.43	645	26020.70	131924933.2	6.68859E+11
5820	97	4.042	4.20	750	19754.38	114970510.9	6.69128E+11
6642	110.7	4.613	2.88	822	14885.41	98868904.01	6.56687E+11
9942	165.7	6.904	1.00	3300	20811.00	206902967.7	2.05703E+12
10347	172.5	7.185	0.91	405	2303.57	23835015.5	2.46621E+11
12073	201.2	8.384	0.59	1726	6401.54	77283215.03	9.33009E+11
12973	216.2	9.009	0.49	900	2754.61	35734416.67	4.63568E+11
14620	243.7	10.15	0.38	1648	3893.71	56926835.45	8.32282E+11
15981	266.4	11.1	0.29	1361	2463.35	39366797.27	6.29121E+11
16879	281.3	11.72	0.25	898.2	1427.17	24089486.73	4.06611E+11
19537	325.6	13.57	0.17	2658	2814.79	54993143.43	1.07441E+12
			SUM	19537	286799988.48	1.78561E+11	2.08811E+14

Table A.5
Data for 14.5 % moisture content experiment

Time			Conc	delt	Ci delt	ti Ci delt	ti2 Ci delt
mins	hrs	days	ppm				
0	0	0	120789.91	-			
15	0.25	0.01	128366.17	15	12088163.96	181322459.36	2719836890
30	0.5	0.021	129980.03	15	12240140.01	367204200.45	11016126013
45	0.75	0.031	123829.02	15	11660903.30	524740648.55	23613329185
60	1	0.042	115588.44	15	10884892.76	653093565.49	39185613930
90	1.5	0.063	102354.21	30	19277266.05	1734953944.71	1.56146E+11
120	2	0.083	89750.74	30	16903544.77	2028425372.89	2.43411E+11
150	2.5	0.104	78265.67	30	14740459.66	2211068949.19	3.3166E+11
180	3	0.125	68170.12	30	12839077.12	2311033880.79	4.15986E+11
210	3.5	0.146	59473.58	30	11201180.89	2352247987.61	4.93972E+11
240	4	0.167	51872.15	30	9769537.89	2344689094.10	5.62725E+11
270	4.5	0.188	44863.61	30	8449558.05	2281380673.60	6.15973E+11
300	5	0.208	38947.76	30	7335372.75	2200611824.77	6.60184E+11
330	5.5	0.229	34912.82	30	6575437.02	2169894214.97	7.16065E+11
360	6	0.25	31519.40	30	5936324.45	2137076801.09	7.69348E+11
425	7.083	0.295	24988.01	65	10196791.76	4333636498.90	1.8418E+12
480	8	0.333	21240.84	55	7334203.34	3520417603.79	1.6898E+12
540	9	0.375	18231.88	60	6867539.91	3708471550.80	2.00257E+12
600	10	0.417	16490.00	60	6211411.31	3726846785.77	2.23611E+12
690	11.5	0.479	15061.14	90	8509788.87	5871754317.63	4.05151E+12
780	13	0.542	13462.57	90	7606574.11	5933127803.56	4.62784E+12
1215	20.25	0.844	11456.40	435	31286423.04	38013003996.58	4.61858E+13
1380	23	0.958	10014.32	165	10373466.22	14315383376.73	1.97552E+13
1500	25	1.042	9440.50	120	7112048.84	10668073261.22	1.60021E+13
1740	29	1.208	7947.90	240	11975182.03	20836816733.98	3.62561E+13
1920	32	1.333	6903.91	180	7801643.73	14979155968.89	2.876E+13
2160	36	1.5	5550.78	240	8363416.87	18064980431.88	3.90204E+13
2400	40	1.667	4391.85	240	6617245.21	15881388503.51	3.81153E+13
2640	44	1.833	3218.50	240	4849346.79	12802275530.45	3.3798E+13
2880	48	2	2135.89	240	3218167.26	9268321702.45	2.66928E+13
3180	53	2.208	506.12	300	953227.18	3031262429.69	9.63941E+12
3240	54	2.25	297.20	60	111948.04	362711652.24	1.17519E+12
3360	56	2.333	133.20	120	100346.45	337164063.86	1.13287E+12
3480	58	2.417	73.56	120	55413.64	192839457.51	6.71081E+11
3600	60	2.5	47.12	120	35499.52	127798285.62	4.60074E+11
3720	62	2.583	37.24	120	28055.77	104367474.41	3.88247E+11
3840	64	2.667	31.28	120	23564.57	90487952.31	3.47474E+11

Table A.5
Data for 14.5 % moisture content experiment

Time			Conc	delt	Ci delt	ti Ci delt	ti2 Ci delt
mins	hrs	days	ppm				
4080	68	2.833	20.12	240	30318.32	123698762.20	5.04691E+11
4200	70	2.917	17.31	120	13038.32	54760930.35	2.29996E+11
4320	72	3	13.91	120	10475.63	45254715.99	1.955E+11
4440	74	3.083	14.31	120	10782.32	47873498.86	2.12558E+11
4560	76	3.167	11.30	120	8515.93	38832622.90	1.77077E+11
5025	83.75	3.49	8.41	465	24559.37	123410818.72	6.20139E+11
5040	84	3.5	8.33	15	784.44	3953579.70	19926041695
5100	85	3.542	8.85	60	3331.71	16991735.99	86657853538
5160	86	3.583	8.57	60	3227.18	16652274.18	85925734762
5280	88	3.667	19.03	120	14334.46	75685971.00	3.99622E+11
5295	88.25	3.677	18.20	15	1713.88	9075009.73	48052176513
5340	89	3.708	16.04	45	4530.72	24194069.73	1.29196E+11
5400	90	3.75	13.95	60	5254.65	28375119.92	1.53226E+11
5465	91.08	3.795	11.32	65	4619.32	25244596.74	1.37962E+11
5520	92	3.833	9.61	55	3316.49	18307018.66	1.01055E+11
5580	93	3.875	8.18	60	3082.16	17198475.46	95967493076
5640	94	3.917	7.19	60	2707.37	15269566.22	86120353506
5700	95	3.958	6.65	60	2503.96	14272594.92	81353791023
5760	96	4	6.29	60	2368.36	13641754.19	78576504121
6005	100.1	4.17	5.47	245	8409.56	50499418.31	3.03249E+11
6285	104.8	4.365	4.85	280	8516.68	53527330.21	3.36419E+11
7025	117.1	4.878	1.85	740	8594.39	60375566.93	4.24138E+11
7490	124.8	5.201	1.84	465	5369.00	40213801.76	3.01201E+11
8540	142.3	5.931	1.56	1050	10315.87	88097564.82	7.52353E+11
9250	154.2	6.424	1.41	710	6301.72	58290934.42	5.39191E+11
10030	167.2	6.965	1.34	780	6539.79	65594045.94	6.57908E+11
10270	171.2	7.132	1.34	240	2025.02	20797002.04	2.13585E+11
10510	175.2	7.299	1.35	240	2031.78	21354014.42	2.24431E+11
11914	198.6	8.274	0.68	1404	5984.03	71293766.41	8.49394E+11
12154	202.6	8.44	0.66	240	995.61	12100643.89	1.47071E+11
12394	206.6	8.607	0.64	240	960.11	11899645.60	1.47484E+11
13604	226.7	9.447	0.40	1210	3021.23	41100783.04	5.59135E+11
13844	230.7	9.614	0.37	240	554.73	7679661.48	1.06317E+11
15907	265.1	11.05	0.31	2063	4002.92	63674517.00	1.01287E+12
16147	269.1	11.21	0.27	240	402.05	6491910.24	1.04825E+11
16387	273.1	11.38	0.23	240	348.23	5706459.14	93511745954
16599	276.7	11.53	0.41	212	541.99	8996462.46	1.49332E+11

Table A.5
Data for 14.5 % moisture content experiment

Time			Conc	delt	Ci delt	ti Ci delt	ti2 Ci delt
mins	hrs	days	ppm				
16839	280.7	11.69	0.41	240	618.01	10406726.82	1.75239E+11
17079	284.7	11.86	0.39	240	594.61	10155260.53	1.73442E+11
19357	322.6	13.44	0.26	2278	3677.99	71194864.11	1.37812E+12
19597	326.6	13.61	0.34	240	515.27	10097835.93	1.97887E+11
19837	330.6	13.78	0.26	240	385.71	7651340.78	1.5178E+11
20392	339.9	14.16	0.21	555	734.34	14974712.54	3.05364E+11
20512	341.9	14.24	0.18	120	139.29	2857217.12	58607237548
20632	343.9	14.33	0.20	120	149.00	3074164.03	63426152268
20752	345.9	14.41	0.28	120	207.53	4306584.69	89370245582
20872	347.9	14.49	0.21	120	159.29	3324616.71	69391400037
20992	349.9	14.58	0.21	120	158.87	3335007.16	70008470238
21442	357.4	14.89	0.20	450	575.08	12330803.61	2.64397E+11
21562	359.4	14.97	0.20	120	148.72	3206695.69	69142772466
21682	361.4	15.06	0.20	120	147.82	3205029.17	69491442527
21802	363.4	15.14	0.19	120	143.20	3122106.14	68068158044
21922	365.4	15.22	0.19	120	142.49	3123764.34	68479161830
22042	367.4	15.31	0.19	120	140.69	3101039.82	68353119626
22222	370.4	15.43	0.11	180	127.86	2841207.41	63137311148
22342	372.4	15.52	0.10	120	77.22	1725199.03	38544396826
22462	374.4	15.6	0.11	120	81.73	1835740.48	41234402661
22582	376.4	15.68	0.11	120	86.24	1947364.53	43975385896
22703	378.4	15.77	0.11	121	86.21	1957188.99	44434061613
22822	380.4	15.85	0.12	119	86.28	1969191.43	44940886730
23662	394.4	16.43	0.09	840	496.67	11752129.79	2.78079E+11
23782	396.4	16.52	0.09	120	69.42	1650950.39	39262902091
23902	398.4	16.6	0.10	120	75.70	1809281.61	43245448955
24022	400.4	16.68	0.10	120	76.22	1831010.63	43984537409
24142	402.4	16.77	0.10	120	77.47	1870220.15	45150854750
24262	404.4	16.85	0.11	120	79.16	1920484.70	46594799747
25446	424.1	17.67	0.09	1184	699.08	17788870.53	4.52656E+11
25566	426.1	17.75	0.10	120	75.14	1921150.95	49116145235
25686	428.1	17.84	0.11	120	81.50	2093467.16	53772797380
25806	430.1	17.92	0.11	120	85.40	2203805.26	56871398465
25926	432.1	18	0.12	120	87.79	2275992.16	59007372621
26046	434.1	18.09	0.12	120	88.02	2292557.70	59711957873
27539	459	19.12	0.12	1493	1136.87	31308289.06	8.62199E+11
27759	462.7	19.28	0.12	220	159.06	4415227.93	1.22562E+11

Table A.5
Data for 14.5 % moisture content experiment

Time			Conc	delt	Ci delt	ti Ci delt	ti2 Ci delt
mins	hrs	days	ppm				
28019	467	19.46	0.12	260	198.51	5561987.90	1.55841E+11
28259	471	19.62	0.11	240	164.59	4651074.13	1.31435E+11
28520	475.3	19.81	0.10	261	172.03	4906403.21	1.39931E+11
28760	479.3	19.97	0.11	240	159.47	4586238.38	1.319E+11
29000	483.3	20.14	0.11	240	159.60	4628267.93	1.3422E+11
29240	487.3	20.31	0.10	240	155.32	4541676.78	1.32799E+11
32944	549.1	22.88	0.09	3704	2021.76	66604751.46	2.19423E+12
33184	553.1	23.04	0.09	240	129.99	4313457.38	1.43138E+11
33424	557.1	23.21	0.09	240	129.41	4325351.95	1.44571E+11
33664	561.1	23.38	0.08	240	126.86	4270479.00	1.43761E+11
34301	571.7	23.82	0.08	637	333.65	11444546.96	3.92559E+11
34541	575.7	23.99	0.08	240	123.40	4262229.90	1.47222E+11
34781	579.7	24.15	0.08	240	123.18	4284168.74	1.49008E+11
35021	583.7	24.32	0.08	240	119.79	4195276.41	1.46923E+11
			SUM	35021	299774130.9	2.11468E+11	3.40374E+14

APPENDIX B

**PREPARATION OF STANDARDS
FOR
GAS CHROMATOGRAPHY ANALYSIS**

PREPARATION OF STANDARDS FOR GAS CHROMATOGRAPHY ANALYSIS

To authenticate the response of the gas chromatograph it is important to develop a standard curve for each detector and for each set of data. Standard curves were developed on all days of sampling. The standards for the TCD were prepared by injecting neat liquid carbon tetrachloride in a sealed steel canister of known volume. The liquid will then volatilize and the concentration of the resulting vapor can be calculated using the following equation:

$$C = \frac{22.4 * 10^6 * \frac{T}{273^{\circ}\text{K}} * \frac{760\text{mm Hg}}{P} * V_L}{V * \text{M.W}} \quad (\text{B.1})$$

Where

C = Concentration in the vapor phase, ppm;

$22.4 * 10^6$ = Avagadro's number;

T = absolute temperature, $^{\circ}\text{K}$;

P = system pressure, mm Hg;

V_L = Volume of liquid carbon tetrachloride added, uL;

V = Volume of canister, L; and

M.W = Molecular weight of carbon tetrachloride, gm/mol (Nelson *et al.*, 1992).

TCD STANDARDS

For the TCD analysis all concentrations >50,000 ppm were analyzed at 'low sensitivity', while those <50,000 ppm were analyzed at 'high sensitivity'. All standards were prepared in 1 L steel canisters by injecting neat carbon tetrachloride. The canisters were sealed at one end using a 5 cm stainless steel nut while at the other end they were connected to a two-way stainless steel valve. After injecting the neat liquid carbon

tetrachloride, the canisters were placed in an oven at 100°C for an hour to allow complete volatilization and uniform mixing. Subsequently the canisters were immersed in a water bath maintained at 100°C for at least 1 hour. By doing so the vapors in the canister will begin to expand and this built-up pressure is then used to inject three vapor samples into the GC. The flow rate for the 3 injections ranged between 450 -250 mL/min. For the ‘low sensitivity’ the concentration range was 48,500, 72,700 and 12,120 ppm. Based on equation B.1, 160, 240 & 400 uL of neat liquid carbon tetrachloride were added used. For the ‘high sensitivity’ segment of the TCD, concentrations of 24,200 ppm, 36,300 ppm and 48,500 ppm were prepared. The amount of liquid carbon tetrachloride injected for these concentrations was 80, 120 and 160 uL respectively. Calibration of the lower region of the TCD (between 10,000 and 13.7 ppm) was conducted using dilutions of factory standards. The procedure for these dilutions is presented in the following section.

FID/ ECD STANDARDS

For all samples below 10,000 ppm dilutions of vapor phase factory standards were prepared. Factory certified concentrations of 10,000, 500 and 0.521 ppm were purchased from Scott Specialty Gases Inc. Stainless steel dilution bottles (10 L from Air Liquide, Canada) were used for all dilution standards. Dilutions were made from these concentrations in dilution bottles.

The concentration of this diluted standard in the mixture was then calculated using the following expression:

$$C_1 = \frac{P_2 * C_2}{P_1 + 13.457} \quad (D.2)$$

Where

C_1 = final concentration of the standard in the dilution bottle, ppm;

P_1 = pressure at which certified standard is transferred into the dilution bottle, psi;

P_2 = final pressure of the mixture, psi;

C_2 = concentration of the certified standard, ppm; and

13.457 = is the correction made for atmospheric pressure, psi.

A stainless steel dilution tank is purged clean by filling it with compressed air, then vacuuming it and allowed to come to atmospheric pressure. A small amount of the certified standard (C_2) was added to the clean dilution bottles at a low known pressure (P_1). Compressed air devoid of any traces of carbon tetrachloride was then transferred to the tank. The transfer was conducted in several stages in order to prevent the heating of the gas mixture. After the transfer was completed, the tanks were placed on a hot plate and heated on high for 30 min, in order to facilitate appropriate mixing. The tanks were then taken off the hotplate and allowed to come to room temperature. The final pressure was then recorded (P_2).

APPENDIX C

PRINCIPLE OF OPERATION OF GC DETECTORS

Principle of operation of Thermal Conductivity Detector (TCD)

The thermal conductivity detector (TCD) contains a heated filament. The carrier gas flows past the filament cooling it and creating a baseline voltage. Due to their different velocities and masses, sample molecules will cool the filament differently from the carrier gas. This causes a change in resistance to the filament. The normal sensitivity of the TCD will vary substantially with the carrier gas used; the flow rate and the detector block temperature. The TCD operates in a thermal balance; therefore its output is very sensitive to changes in gas flows. Sensitivity ranges between 10 and 128,982 ppm (saturation concentration for carbon tetrachloride at 21.8 C)

Principle of operation of Flame Ionization Detector (FID)

The flame ionization detector (FID) detects compounds that produce ions when burned in an H₂-air flame (includes most organic compounds). These include almost all organic compounds. Several compounds produce very little response such as CO, NO and NH₃. The response is linear for most compounds and the signal is very stable owing to an ease of operation. Sensitivity ranges between 2.25 and 500 ppm.

Principle of operation of Electron Capture Detector (ECD)

The electron capture detector (ECD) contains ⁶³Ni, which emits beta particles. The particles collide with makeup gas (N₂) and result in a chain reaction, which produces many more lower energy electrons. The electrons are then captured by electronegative sample substituents. The free electrons are removed by a pulsing current and this current is compared to a reference. The currents are set equal by fluctuating the pulse frequency. The frequency is converted to a linear signal. The signal is dependent upon the electron

removal occurring in the cell. The detector responds best to halogen and oxygen containing molecules with increasing sensitivity exhibited with the numbers of these atoms contained within the substance. Sensitivity ranges between 50 and 1250 ppb.

APPENDIX D

PRINCIPLE OF OPERATION OF ACCELERATED SOLVENT EXTRACTOR

The ASE® 200 Accelerated Solvent Extractor is an automated system for extracting organic compounds from a variety of solid and semisolid samples. It accelerates the traditional extraction process by using solvent at elevated temperatures. Pressure is applied to the sample extraction cell to maintain the heated solvent in a liquid state during the extraction. After heating, the extract is flushed from the sample cell into a standard collection vial and can be analyzed on a GC. The sample is packed in a stainless steel extraction cell between two sand layers and then loaded in the instrument along with the VOA collection vials. Figure D.1 provides a schematic of the extraction process.

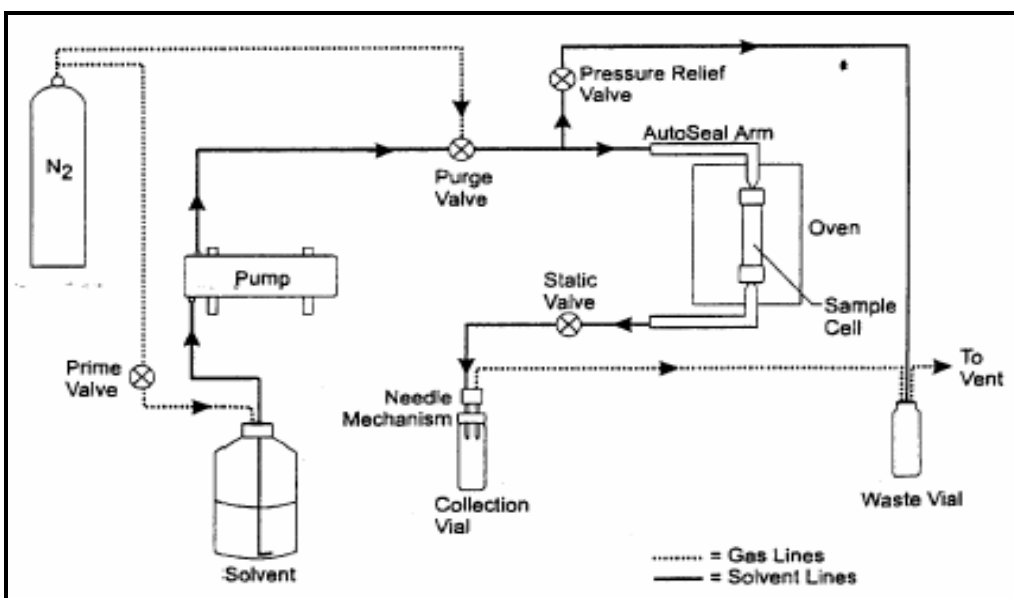


Figure D.1 – Schematic of Accelerated Solvent Extraction.

When the method is started the auto seal arms transfers the cell into the oven where pressure is applied to seal the cell. The pump begins pumping solvent into the cell. When the cell is full and the collection vial contains about 1 mL of solvent, the static valve closes and flow stops. The cell is heated for a fixed time to ensure that the sample reaches thermal equilibrium. The static period then occurs where the static valve opens periodically to maintain the set point pressure in the cell. Next flushing occurs where the

extract flows into the collection vial. Fresh solvent is pumped through the cell (66% of the cell volume).

The remaining solvent is displaced with purge gas (N_2). The collection vial now contains all of the solvent and the analytes extracted from the sample. Residual pressure is released from the extraction cell. Pressure is vented from the system. The cell is unloaded from the oven and returned to the tray. The needle mechanism is removed from the vial. The trays advance to their next positions and the next run starts.